FROM THE SEASHORE TO THE STRATOSPHERE. A STEP CLOSER TO CONTINUOUS LUNG MONITORING USING WEARABLE ULTRASOUND

J.M. Visser

FROM THE SEASHORE TO THE STRATOSPHERE. A STEP CLOSER TO CONTINUOUS LUNG MONITORING USING WEARABLE ULTRASOUND. LUNG SLIDING QUANTIFICATION

- Master Thesis -

Jeffrey Martin Visser

Student number : 4362810

March 2022

Thesis in partial fulfilment of the requirements for the joint degree of Master of Science in

Technical Medicine

Leiden University | Delft University of Technology | Erasmus University Rotterdam

Master thesis project (TM30004 ; 35 ECTS)

Dept. of Intensive Care, LUMC

May 2021 – March 2022

Supervisor(s):

drs. J.E. Lopez Matta, LUMC
dr. D. van Westerloo, LUMC
dr. C. Elzo Kraemer, LUMC
drs. A. Schoe, LUMC
dr. ir. H. Pham, Philips Research
ir. J. Haartsen, Philips Research

Thesis committee members:

Prof. dr. E. de Jonge, LUMC (chair)
Prof. dr. Ir. R. Dekker, TU Delft
dr. D. van Westerloo, LUMC
dr. ir. H. Pham, Philips Research

1. Preface

Congratulations, you received a copy of my master thesis that I conducted in the intensive care department of Leiden University Medical Center (LUMC). It was a great opportunity to study all the ins and outs in both medical and technical fields during the last six years and to complete this journey in collaboration with a high tech medical company and a medical center.

My academic study career started with the study Electrical Engineering. Although it was a very nice study, I was missing something. My girlfriend was studying Medicine and I was somewhat envying her. Thus, I decided to participate in the selection for the study Clinical Technology, a one year old study from TU Delft, Erasmus University Rotterdam and Leiden University that combines medicine with technology. It turned out to be the perfect study for me.

The first aim of this project was to investigate if the possibilities of continuous ultrasound monitoring may be valuable for the critical care. I decided to continue with lung monitoring because we had a lot of COVID patients admitted to the hospital at the start of the graduation internship. Philips research made me very enthusiastic about a new type of ultrasound 'patches'. I immediately understood the added value and I wanted to work with it as an early adopter. Unfortunately, the manufacturing process is still not completed at the end of this thesis. Later, we rewrote the aim to what later could be used with the ultrasound patches.

It was a long way with a lot of failures and successes. I have learned a lot and really enjoyed working in the intensive care with very driven people. Moreover, it was a mind-blowing new world at Philips where I learned all new business related disciplines. This includes a new vocabulary with words like, 'Value streams', 'agile' and other abbreviations (Did, you know these words, Medic's?). All the members of the patient monitoring, ultrasound teams, and all the Philips interns were very kind and helpful to me.

I like to express my sincere appreciation to my supervisors for helping me shape this research, giving me the fruitful ideas and for all the time they invested into reviewing my work; thanks David, Jorge and Carlos. I want to thank Bram for his helpful insights and discussions, mostly on the ventilator. You gave me the courage to start, and really like your enthusiasm about this project. I want to thank Jaap, Oleh, Willem, Roberto, and Deep for your really valuable discussions on this project and the feedback you gave me. Jaap, you were my first contact person for my technical questions and you were always available. Finally, I would like to thank Hoa. You are a real bridge maker, connecting all valuable members to this project. you embrace this project and bring it to attention. Hopefully, once completed, we can bring this project to reality.

More appreciations go out to my family and girlfriend, who listened endlessly to my stories on lung monitoring and supported me, thank you!

My student time is over. It is time for a new adventure!

J.M. Visser

Leiden, March 2022

2. Abstract

Background: The prevention of ventilator-induced lung injury (VILI) is an important topic in critical care. Lung overdistention is a great attributor to VILI. Regional evaluation of the pulmonary mechanics is a relatively new method and is currently being studied using electrical impedance tomography (EIT) and computed tomography (CT). However, ultrasonography may be an effective alternative to measure lung overdistention by quantifying lung sliding.

Objective: The primary aim of this study was to explore if lung sliding can be quantified using in-house made speckle tracking algorithms. Second, the usability of lung sliding quantification to detect lung overdistention was investigated.

Method: Two speckle tracking algorithms were built and validated to quantify lung sliding. Adult patients admitted to the ICU were prospectively examined using ultrasound. Ultrasound images were analyzed offline using the in-house developed Fourier-Based Speckle Tracking algorithm (FBST) and the Intensity-Based Speckle Tracking algorithm (IBST). The performance of the best algorithm was validated against the manual evaluation of lung sliding by experts and validated against lung compliance. Besides, the performance of the best algorithm was investigated by reproducibility testing. Finally, we tested the algorithm for its ability to detect lung overdistention.

Results: The FBST algorithm could not reliably quantify lung sliding and was not further evaluated. However, the IBST algorithm showed an overall success rate of 88%. Moreover, the IBST algorithm differentiated normal and moderate lung sliding with a mean IBST score of 12.1 and 29, respectively ($p<0.001$). A positive correlation was measured between IBST score and lung compliance (β 0.15, SE 0.025, 95% CI 0.101-0.208, $p <0.001$). The reproducibility test calculated a relative standard error of 2.7. Finally, a difference was found in IBST scores between patients with a PEEP value <12 and ≥12 with a mean ± SD of 20.9 ± 7 and 12.6 ± 6, $p < 0.05$, respectively.

Conclusion: The IBST algorithm enables a robust lung sliding quantification. The IBST scores correlate well with expert opinion and lung compliance, but the reliability needs improvement. Our results show that detection of lung overdistention using ultrasound is feasible. Further clinical studies should assess if ultrasonography can measure lung overdistention.

Contents

3. List of abbreviations

Abbreviation	Explanation
ANOVA	Analysis of variance
ARDS	Acute respiratory disease syndrome
ASV	Adaptive support ventilation
AUC	Area under the curve
CI	Confidence interval
CMUT	Capacitive micromachined ultrasonic transducer
COVID-19	Coronavirus disease 2019
CT	Computed tomography
DICOM	Digital imaging and communications in medicine
EIT	Electrical impedance tomography
etCO2	End tidal C02
FBST	Fourier based speckle tracking
FFT	Fast Fourier transform
FOV	Field of view
IBST	Intensity-based speckle tracking
ICU	Intensive care unit
LUMC	Leiden university medical center
LUS	Lung Ultrasound
NCC	Normalized cross correlation
p-CMV	Pressure controlled mandatory ventilation
PEEP	Positive end-expiratory pressure
PMDS	Patient Data Management System
POCUS	Point Of Care Ultrasound
SDC	Speckle decorrelation
SE	Standard error
ST	Speckle tracking
US	Ultrasound
VILI	Ventilator induced lung injury

4. Introduction

4.1 Clinical need

Severe respiratory failure happens when gas exchange is compromised by underlying lung abnormalities, such as consolidations, atelectasis, or a compound of these in what is known as the acute respiratory distress syndrome (ARDS). Many of these patients end up mechanically ventilated to keep them alive but paradoxically this mechanical ventilation can also potentially harm the lung even further resulting in ventilator-induced lung injury (VILI) (1). VILI is caused by a combination of factors including alveolar overdistention from excessive tidal volumes (volutrauma) and opening and closing of alveoli (atelectotrauma) (2). Recruitment maneuvers as well as applying positive end expiratory pressure (PEEP) may provide significant benefit by reducing the latter traumas. However these maneuvers are not indolent and cause potential further damage in the form of overextension to healthier parts of the lung. This regional overdistention is linked to the aforementioned volutrauma and barotrauma with possible activation of cytokine storms resulting in multi-organ dysfunction (3).

The effective aim of lung protective mechanical ventilation is to determine the ventilator setting that maximally opens the parts of the lung that are closed without overextension of the parts that are still open. The critical care community is constantly searching for ways to achieve this utopic form of ventilation. For instance, the measurement of esophageal pressure as a surrogate of pleural pressure has been studied as a tool to prevent VILI (4). Although this technique may lead to a better understanding of actual trans pulmonary pressures during mechanical ventilation it does not assess regional overdistension due to the intrinsic heterogeneity of acute lung injury.

Lung imaging has also been studied. As of now, reliable data regarding the regional differences in the lung may only be gathered by way of serial CT scanning or electrical impedance tomography (EIT) measurements. Serial CT scan is limited by the required mobilization of these critically ill patients and the risk involved in the latter, while EIT requires additional tools not readily available to all intensive care units. We believe that ultrasonography may be an effective alternative without the limitations of the aforementioned techniques. One example of the potential of ultrasound to better understand the actual pulmonary status is B-line quantification algorithms.

4.2 Lung Ultrasound(LUS) and POCUS

Ultrasonography is an imaging modality dating back to 1963 when the initial B mode ultrasound devices were constructed. A two-dimensional image gave the examiner the possibility to look inside the human body without radiation. In the mid-seventies, the devices were able to create a real-time two-dimensional view that identified dynamic properties of tissues. The transducer transmits a soundwave pulse through the body and subsequently receives the echoed sound waves. By way of sound wave transmission, reflection, and impedance transmissions, images are generated and tissues are differentiated (5). Later, more advanced devices were implemented that integrated Doppler effect techniques for visualizing and quantification of blood flow (6).

Ultrasound devices are constantly improving. For instance, because transducers are smaller and more portable, attachment to phones and tablets is feasible and accessible. Ultrasound examinations presently are not limited by departmental location and can be performed at the bedside. This new method is called point-of-care ultrasound or POCUS. Doctors in acute scenarios can directly test specific pathological hypotheses to reach a fast and correct diagnosis.

One of the applications of POCUS is the use of bedside lung ultrasound in emergency settings. Liechtenstein et al. first described the use of ultrasound to diagnose acute pulmonary pathology in the so called “BLUE” protocol (7). This was the first time lung ultrasound was recognized as a valuable diagnostic tool since before then it was assumed that given the air filled nature of the lung ultrasound of the lung was not feasible. The BLUE protocol is based on three measurements: First, the number of

B-lines represents comet trail artifact on imaging which is indicative of fluid infiltration between the lung parenchyma and the pleurae. Horizontal A-lines reside beneath the pleural line and represent correct aeration and is therefore a feature of normal lung. Second, pleural movement is scored by the presence or absence of lung sliding and the morphology of the pleurae (normal thickened or fraying). Third, the presence of lung consolidations (non-ventilated areas) are depicted as liver-like tissue in imaging. Lung ultrasound scoring systems reflecting the level of atelectasis and consolidations in different areas of the lung and therefore providing a better understanding of regional differences. These simple measurements could detect various types of diagnoses with high accuracy (7). However, one drawback is that the LUS examination must be performed by a person and not automatically. Therefore, obtaining a continuous measurement over more days is very labor intensive. Examples of lung ultrasound images are depicted in figure 1A, 1B.

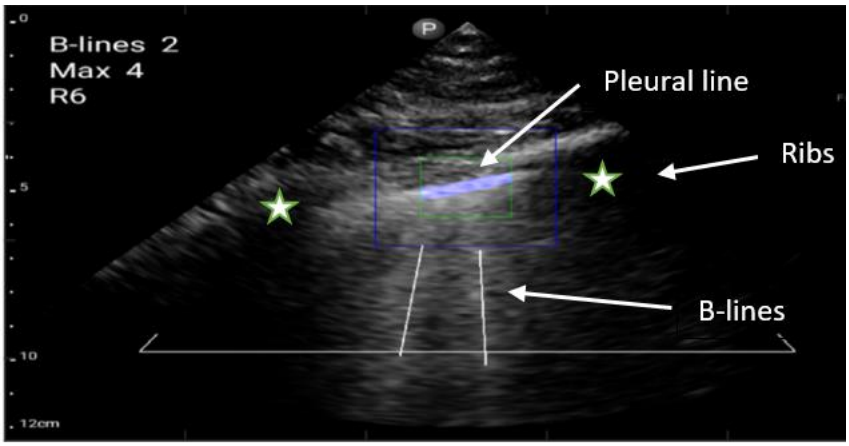

Figure 1A: B-lines extending from pleural line to the bottom of the image. Ultrasonography image is made using a phased array Lumify transducer. Interstitial pulmonary edema accumulates with the number of B-lines. The pleural line is partly colored blue. Ribs are depicted as white stars and are recognizable by the black shadow underneath.

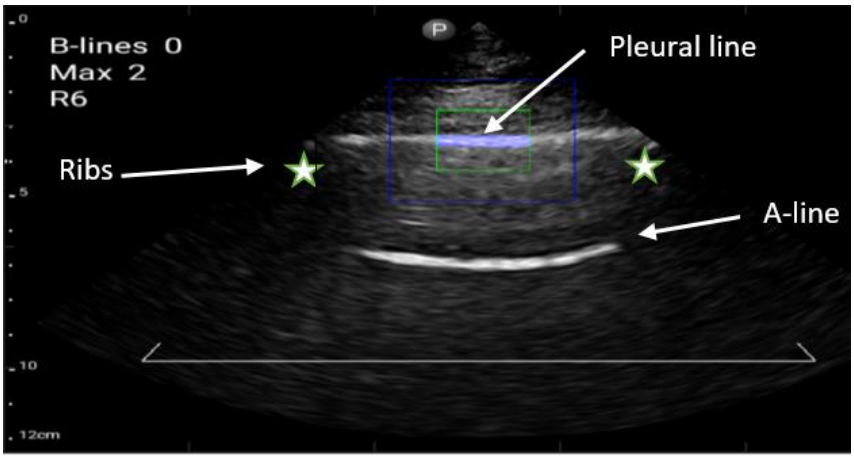

Figure 1B: No B-lines extending from pleural line and the presence of an A-line indicates no interstitial pulmonary edema and correct aeration of the lung.

Several studies hypotheses that a reduction lung sliding could be an indication of lung overdistention. (8, 9) As can described in the BLUE protocol, ultrasound is able to detect lung sliding. Lung sliding can visually be recognized by a dynamic hyperechoic line in the image. This is caused by the visceral pleura that moving against the parietal pleura with respiration. In literature, a first approach to quantify lung sliding is seen in patients with a pneumothorax. However, they used a speckle tracking algorithm used for cardiac strain analysis and only available on GE ultrasound systems. Still, this software cannot be currently used in clinical practice because the software is not intended to quantify lung sliding and

lacks continuous measurement of lung sliding. The results of this study were promising with a perfect detection of pneumothorax patients in a retrospective cohort study. (10) Yet, still no commercial software is available to quantify lung sliding.

4.3 Ventilation optimization as a future goal

Alterations to the ventilation settings are done frequently by the healthcare professionals and are guided by oxygen saturation percentages and the results of blood gas analyses (pH, pO2, pCO2). However, in most hospitals, no strategies are used that may inform clinicians on regional lung ventilation which may lead to overdistention of healthy lung zones. Theoretically, this information may be crucial to ascertain that a safe mechanical ventilation strategy is applied.

Continuous monitoring of lung morphology in ARDS may be of benefit as the regional differences in the lung as well as the overall clinical situation changes continuously over time. Based on a previously performed literature review, the use of Electrical Impedance Tomography (EIT) is bale to measure regional- air distribution, lung overdistention, and lung collapse in real-time. However, EIT has severe limitations as mentioned earlier. We believe that in contrast to EIT, Lung ultrasonography may also be able to provide accurate measurements for alveolar stress, lung movement, and extravascular lung water in real-time with a high spatial resolution but with low costs and high availability.

Our future goal is to integrate lung monitoring solutions with the ventilator. An idea is to integrate multiple transducers to specify information on a regional level of the lung during mechanical

ventilation. Monitoring devices such as ultrasound patches (Appendix A4) may be able to provide continuous lung ultrasound images in a small form factor. With the use of advanced image processing techniques we may be able to constantly screen for and quantify pulmonary oedema and monitoring of lung sliding may be able to measure lung overdistention continuously. A trained model with these measurements could provide a closed-loop ventilator algorithm that regularly evaluates the ventilator settings and automatically optimizes the ventilation strategy.

4.4 Aim

This thesis aims to explore if lung sliding can be quantified using speckle tracking software without the use of any proprietary software. Next, the functionality will be validated against the manual evaluation of lung sliding by experts and ventilation compliance. Then, we will investigate if the quantification of lung sliding can be used to detect lung overdistention. We hypothesized that an overdistended lung results in a movement reduction during lung sliding, which will be quantified using an in-house developed speckle tracking algorithm (8, 9). The performance of the algorithm will be tested using the clinical data we will collect during this research.

The main goal is divided into the following objectives:

- Developing an algorithm to quantify lung sliding.
- Validating the performance of the lung sliding quantification algorithm using clinical data.
- Investigating implementation of the lung sliding quantification algorithm for prediction of lung overdistention.

This research project will be performed at the Leiden University Medical Center (LUMC) at the Intensive Care department and is a collaboration between the LUMC and Philips Research.

5. Methods

5.1 Data acquisition

Ultrasonographical and ventilation data for this study were acquired prospectively during the study period and were used to validate the algorithm. All patients older than eighteen admitted to the intensive care unit of LUMC were eligible. Included patients were regularly examined with lung sonography using the Ultrasound Targeted OPtimization In Acute lung injury (UTOPIA) protocol. (appendix A3). Patients were excluded if they were not intubated or feeling discomfort during examination. Patients characteristics were obtained from the Patient Data Management System (PDMS).

Our study uses standardized locations of lung ultrasound examination as has been recommended in the study of Dargent et al. (11). There are six areas in each lung. A schematic overview of these locations is depicted in figure 2.

First, zone 1 and 2 are between parasternal line and anterior axillary line. Second, zone 3 and 4 are between anterior axillary line and posterior axillary line. Last, zone 5 and 6 are between posterior axillary line and the posterior median line. Then, the zones are subdivided using the midline of the thorax.

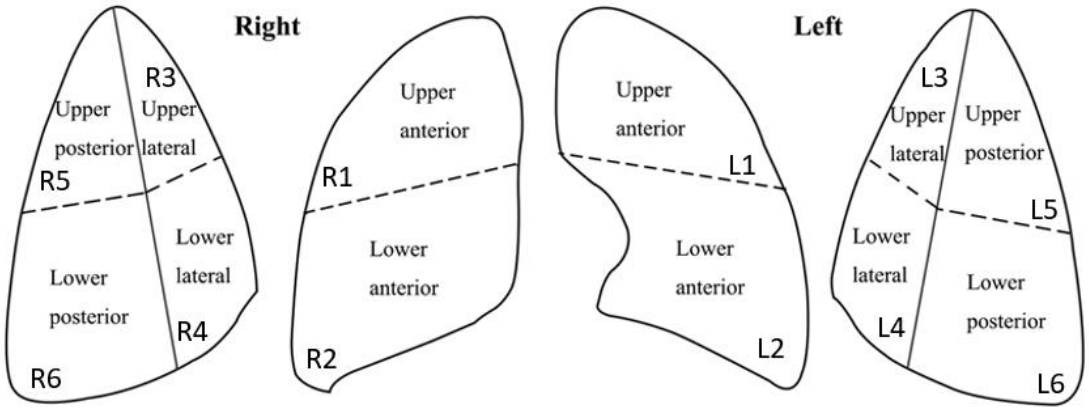

Figure 2: Each lung is separated into six quadrants: anterior, lateral and posterior zones that are further divided in an upper and lower zone. Image from Deng, Q., Cao, S., Wang, H. et al. (12)

We employed the Lumify phased array transducer S4-1 (FOV 90 degree, scan depth: 24 cm, bandwidth 4-1Mhz) in combination with a Samsung galaxy tab and lumify app to perform a complete lung examination. The examinations were made by a trained medical student. Furthermore, we chose to use the B-line quantification feature integrated in the software that guide the sonographer in which order the lung segments need to be examined. The software then annotates the image automatically with corresponding location. Before each examination, the following settings were set: lung preset, clip duration 7 sec, depth 12 cm and gain 49. Each of the 12 lung ultrasound clips are saved as Digital imaging and communications in medicine (DICOM) files, exported with an USB flash drive and pseudonymized. During our Lumify based acquisition protocol a general ultrasonic gel is used.

Ventilation data was collected simultaneously with the ultrasound data. All patients were ventilated using the Hamilton C6 ventilator. Ventilation modes can variate between pressure controlled mandatory ventilation (p-CMV), adaptive support ventilation (ASV), and spontaneous. P-CMV was preferred because the pressure and volume measurements were more predictable. Hamilton memory box dongle was attached to the ventilator and used to log following parameters: tidal volume, pressure, flow, and etCO2. Data was recorded with a sample rate of 100 Hz. After data recording, the data is extracted from the SD card and saved to a secured server. The data of the ventilator were offline linked with the pseudonymized data of the ultrasound data. The ventilator data was not synchronized with the ultrasound measurements. Therefore the time difference of inspiration between ventilation data and ultrasound data cannot retrospectively be determined.

5.2 Building a lung sliding algorithm

For the quantification of lung sliding, this thesis explored two methods. The first method was a Fourier-based block-matching algorithm. This method is also known as the speckle tracking algorithm and generally known in cardiac strain imaging. (13) The second method was a temporal magnitude changes algorithm based on a frame to frame intensity change. The author built both algorithms in MATLAB (2021b, MathWorks, USA).

A. Fourier-based speckle tracking algorithm

The Fourier-based speckle tracking (FBST) uses multiple tracking blocks that can be manually or automatically placed in the lung ultrasound image. Automatic placement of a tracking block is only available when using a pleura segmentation tool. For the purpose of pleura tracking, these blocks are placed on the pleural line. A search window is defined around the target as another block that is two times the size of the tracking block, as depicted in figure 3. Next, the search window is divided into non-overlapping blocks. The algorithm then searches for each tracking block, which is the most similar block within the search window. The search window prevents incorrect locations and lowers computational costs. The motion displacement is measured by the center pixels' location difference between frame T and frame T+1.

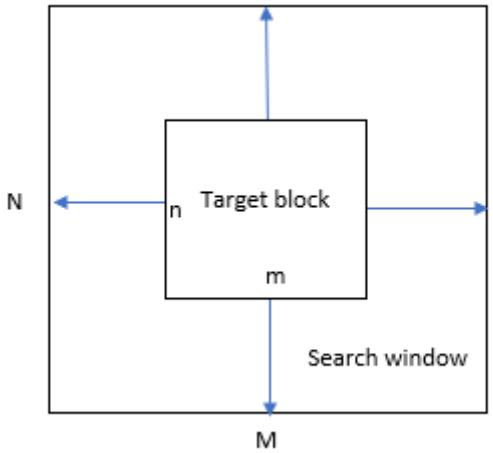

Figure 3: Schematic overview of the search window. N and M are two times the size of n and m.

The similarity measurement of the algorithm uses a normalized cross-correlation (NCC) metric. Several studies found NCC the most stable tracking metric because it normalizes the intensity differences between frames (14). For the metric calculation, we use the cross-correlation theorem used by Garcia et al. depicted in figure 4 (15).

Cross-correlation theorem

- multiplying the Fourier transform of one function by the complex conjugate of the Fourier transform of the other gives the Fourier transform of their correlation

$$f \star g = \mathcal{F}^{-1}(F \times \bar{G})$$

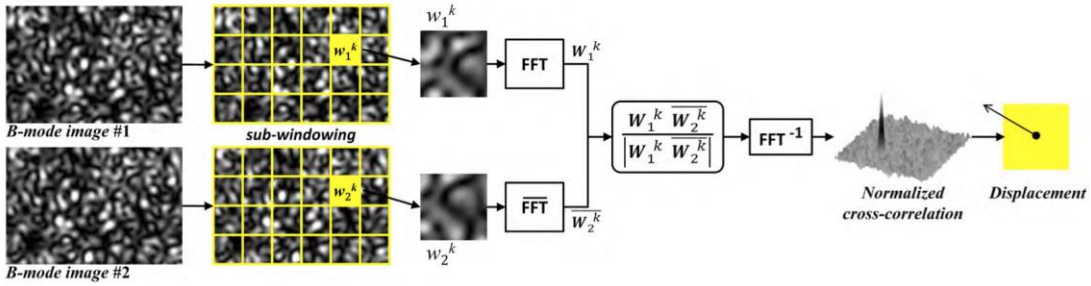

Figure 4: Speckle tracking method using Fourier shift. Illustration by Garcia et al. (15)

The following steps were performed in the algorithm. The graphical representation is depicted in figure 5.

1. Load DICOM image as matrix data and import ventilation data.
2. Calculate the target energy block that is used later for normalization with [M, N] being the size of the target block.

$$\text{Energy\_target} = \sqrt{\sum Target(M,N)^2}$$

3. Rotate the target image 180 degrees. This is equal to the complex conjugate function as described in figure xx.
4. Add zero padding to equalize the dimensions of the target image to the search window.
5. Compute the discrete Fourier transform of the target image using the standard MATLAB function Fast Fourier Transfer (FFT).
6. Repeat step 2-5 for every search block.
7. Compute the discrete Fourier transform of the search window image using the standard MATLAB function FFT.
8. Calculate the energy of the search window block.
9. Calculate the similarity map by:

$$\text{Similarity map} = fft(target) * fft(search\ window\ image)$$

10. Normalize similarity calculation by:

$$\text{Normalized similarity map} = \frac{fft(target) * fft(search\ window\ image)}{Energy_{target} * Energy_{searchwindow}}$$

11. Find the maximum value in the similarity map and determine corresponding coordinates.
12. Move target blocks to new locations.
13. Repeat steps 1-12 for each frame in the acquisition.

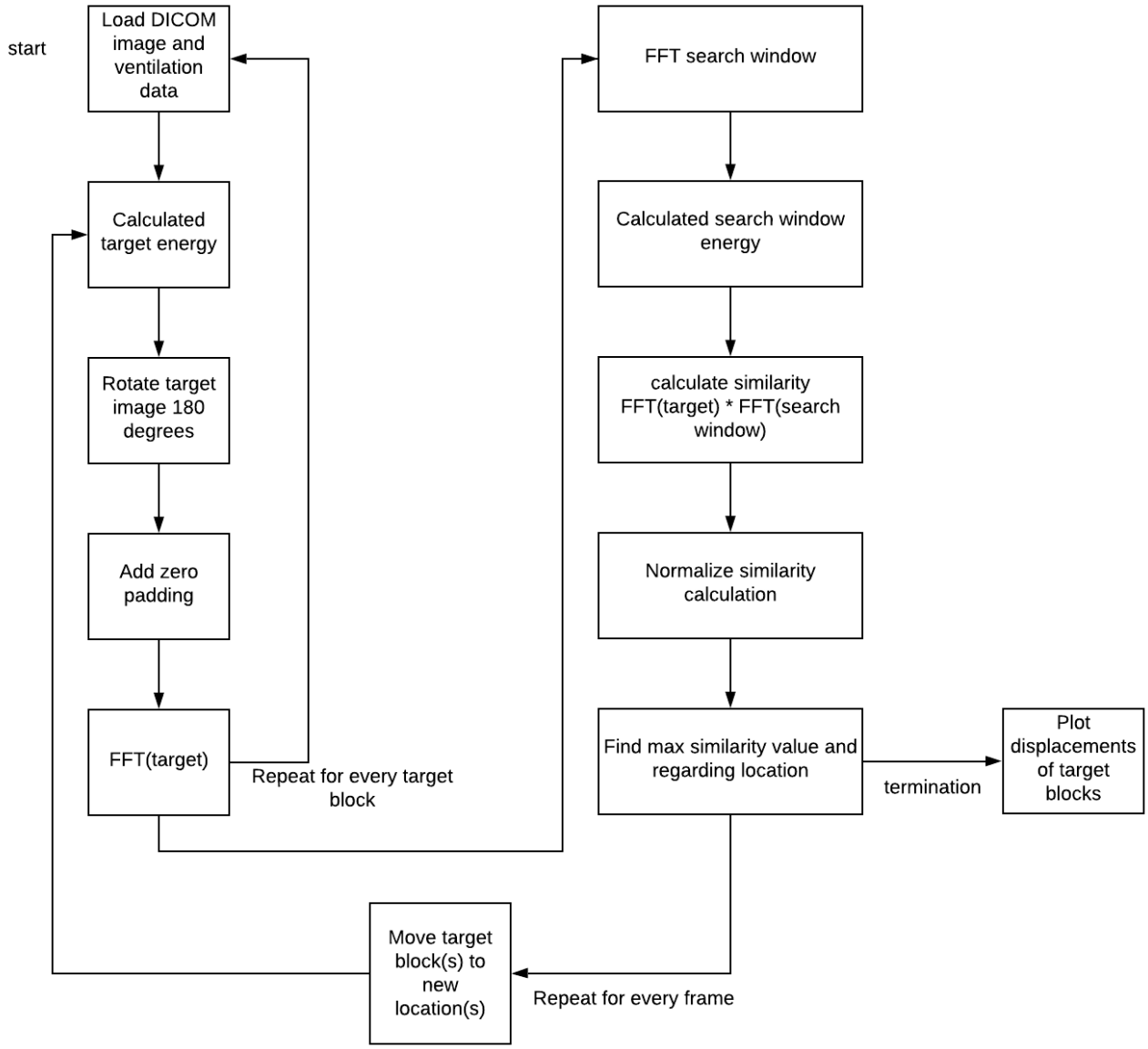

Figure 5: Flowchart FBST algorithm.

After the speckle tracking analysis, the displacement between two blocks are plotted over time. During inspiration, the distance between two blocks should increase whereas expiration should decrease the distance. To evaluate the movability of lung sliding the peak-to-peak value of the displacement was calculated. This value is called FBST score.

B. Intensity-based speckle tracking algorithm

The intensity-based speckle tracking (IBST) algorithm does not determine a direct displacement of the visceral pleural line but calculates the magnitude of intensity changes to estimate the movement of the lung sliding. The displacement could theoretically be estimated by the integral of the velocity measurement.

To start the algorithm, a target block is placed automatically on the pleural line with the upper half of the square filled with muscle tissue, this was done by pleural segmentation. An intensity-based thresholding is performed to separate the hyperechoic structures from the other structures. Besides the pleura, other high intensity structures like muscles will be segmented. However, the pleural line is the most prominent structure. Next, we select the largest segmentation in the image and the center coordinate of that segmentation is determined. The vertical y coordinate of the segmented center coordinate is used as the height of the pleura. Then, the coordinates of the tracking block are placed on the same height of the pleura and below the origin of the ultrasound beam, in the middle of the x axis. The segmentation step is also visually explained in figure 6.

The FBST algorithm as described above is used to track the target block to filter out transducer motion and other artifacts. Each target image of 100x100 pixels is saved in a memory vector. After some executive frames, the algorithm starts with the calculations to determine the movement per pixel resulting in 10,000 signals with intensity values versus time in multiple samples. The Fourier transfer function creates a frequency plot that shows each frequency and its corresponding magnitude. All frequencies above a certain threshold were summed per pixel. A Vesselness segmentation algorithm selects the pixels of the pleura to only measure pleural movement.

The following steps were performed in the algorithm. The graphical representation is depicted in figure 6.

1. Load DICOM image as matrix data and import ventilation data.
2. Select region of interest. Move the target box to the pleural line with the upper half filled with muscle tissue.
3. Save target image matrix to memory.
4. Move the target image to the next location.
5. Take the last saved target images to calculate the frequency plots of all the pixels.
6. Add data regularization operations.
7. Perform automatic segmentation on pleural line by Vesselness2D filter (16).
8. Average all pixels within the pleura segmentation step to define the average value for the pleural movement.
9. Repeat steps 3-9 for each frame in the acquisition.

A final report is created in three steps. First, all LUS DICOM files of one patient are processed. Second, the corresponding lung locations are detected by searching the location annotation in the image. Finally, the graphs of the locations are plotted in alphabetic order. Each plot will show the signal of movability of the pleural line and the ventilator's corresponding flow and pressure data. To summarize the movability of the pleural line in one value, the area under the curve of the movability signal is calculated. This value is called the IBST score.

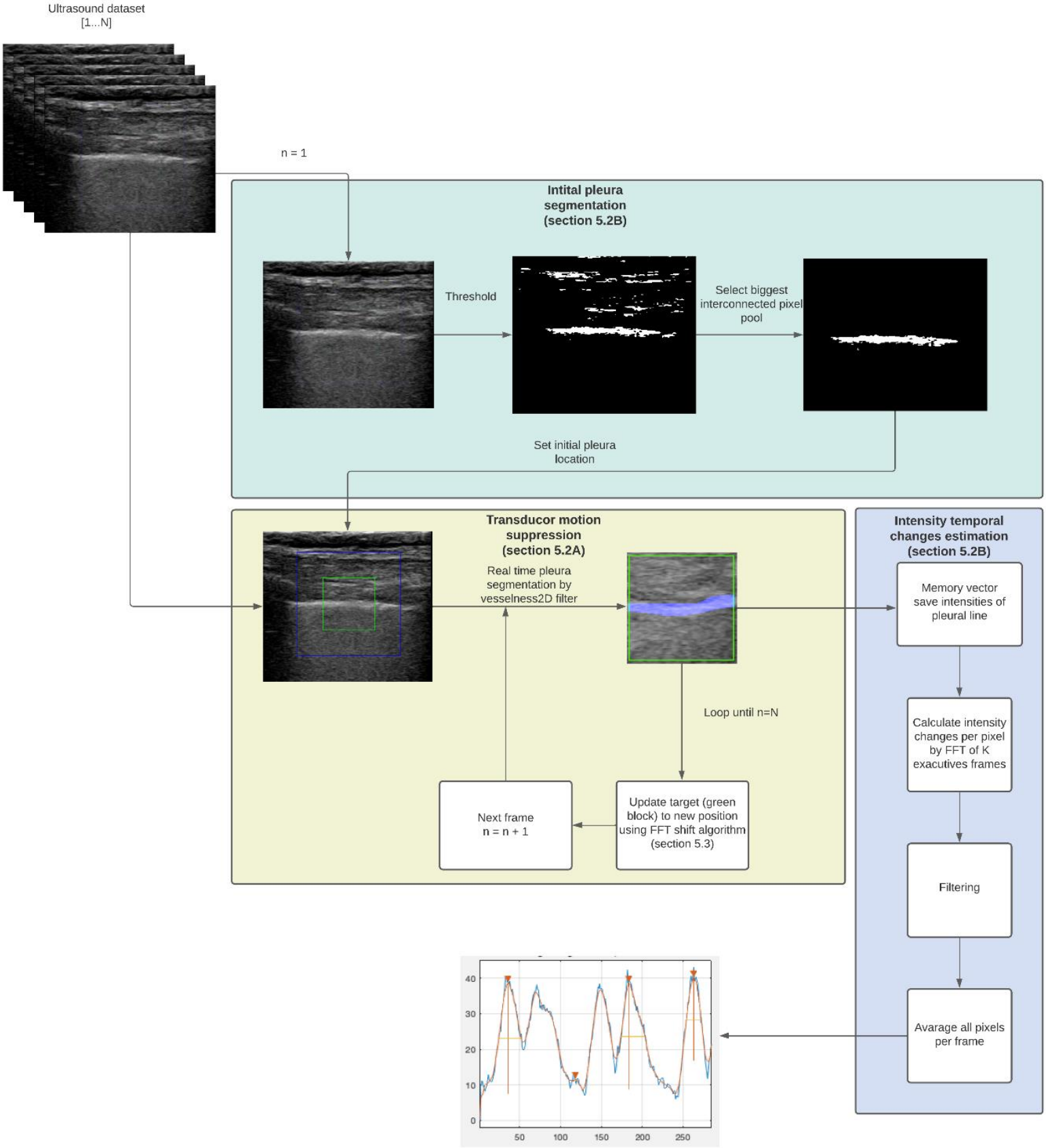

Figure 6: Flow diagram of the IBST algorithm.

5.3 Data analysis

5.3.1 General performance of both algorithms

First, all LUS DICOM files per patient were processed. The ultrasound clips were analyzed offline using the lung sliding algorithms as described in section 5.2. A final report as output depicts all movability scores of the different lung segments. The FBST and IBST algorithms were tested on general performance and their output was visually inspected. Then, the best algorithm was chosen by the author and further assessed in all following steps. Next, we reviewed the success rate of the best algorithm and evaluated the types of errors. The errors were detected by visually inspecting each tracking operation per ultrasound clip. Then, the lung sliding signal produced by the best algorithm was compared with the flow and pressure signal of the ventilator in one patient. Finally, we compared the lung sliding score with a radiological image in another patient.

5.3.2 Validation experiments

A. Expert lung sliding quantification versus lung sliding quantification algorithm

A survey was created to compare the quantified lung movement with expert assessment. We made an easy to work with, web-based survey using Limesurvey. Twenty-three ultrasound images were randomly chosen out the prospectively collected data. Each image was inspected beforehand and excluded if the image had tracking failures. Four lung ultrasonography experts received an email with a link to the survey. The ultrasound clips were visualized to the experts one by one together with the question: 'How would you characterize this pleura?'. Then, the experts were asked to choose one of the following options: no lung sliding, moderate lung sliding, or normal lung sliding. An example is depicted in figure 7. Only the images with more than 75% consensus were analyzed. The images were grouped based on the categorization of the experts. An ANOVA statistical test was used to test the differences of the lung sliding score between the three lung sliding options. Furthermore we calculated the agreement between the raters by following formula:

$$Interobserver\ agreement\ = \left(\frac{Agreements}{Agreements + Disagreements}\right) x\ 100$$

With agreements the total number of ultrasound clips that had 100% consensus between all raters and disagreements the total number of ultrasound clips with less than 100% consensus.

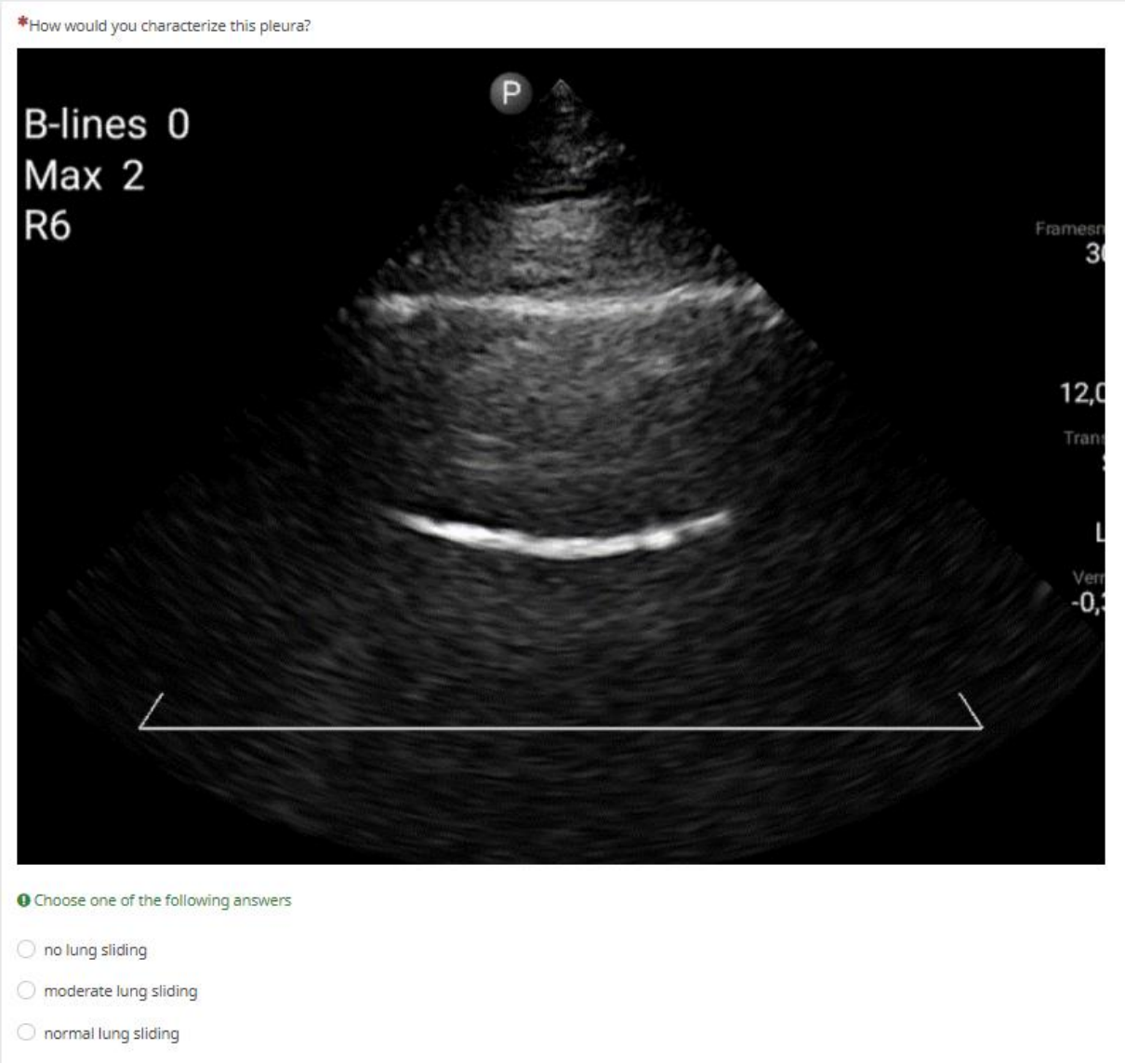

Figure 7: Example question of the lung sliding questionnaire. Ultrasound clips were converted as gif files so they appear as dynamic images on the webpage.

B. Correlation between lung sliding quantification algorithm and lung compliance

The lung compliance experiment uses all patients ultrasound data available at the moment of analysis. Patients ventilated with spontaneous ventilation mode and patients data with more than 25% missing data were excluded from the analysis. Patient data were sorted by unique patient ID to account for repeated measurements. Ventilation compliances values at the time of examination were extracted from the PMCS. The lung sliding score was averaged between all lung segments to match with the global measurement of the lung compliance.

A linear mixed-effect model was used to test the association between lung movement and lung compliance. MATLAB was used to fit the linear mixed-effect model. (17) We used a fixed effect for the lung compliance and a random effect for the patients' unique ID, resulting in the following formula:

$$Lungsliding\ score\ _{average} \sim 1 + Compliance + (1|PatientID)$$

C. Correlation between lung sliding quantification algorithm and overdistention

For lung overdistention experiment we use all patients ultrasound data available at the moment of analysis. PEEP was extracted from the PMCS at the time of examination. The ability to detect overdistention using the lung sliding quantification was tested by dividing patients into two groups. The first group was ventilated with a low PEEP (<12). We proposed that these patients were less prone to lung overdistention because lower PEEP pressure is associated with less lung overdistention. (18) the second group was ventilated with a PEEP 12 or above.

The frontal regions in the lungs are more sensitive for lung overdistention. (19) We average the four frontal regions (L1, L2, R1, R2) for each patient and compare the PEEP groups in mean and standard deviation. Differences were compared using a two sampled t-test for data with a normal distribution and equal variances. Anderson-Darling test was used to test if data was normally distributed. P values <0,05 were considered statistically significant.

5.3.3 Reproducibility of lung sliding quantification

Reproducibility testing is necessary to assess possible fluctuations on the measurement. The ultrasound examination was repeated three times on one patient. Four different lung segments were used (R5, R6, L5, L6). Reposition of the probe was performed with great care to assure the same position. Resulting in a total of twelve ultrasound measures. The patient laid in a supine position and was fully sedated. To account for possible spontaneous breathing, we chose to examine a patient treated with a muscle relaxation agent and ventilated using a pressure-controlled ventilation mode.

A 95% confidence plot was made to visualize the variation of the lung sliding signal. One lung segment was chosen. The three measurements of that lung segment where synchronized by shifting the signals so that the first peak match in time between all three signals. Then, the signal is averaged for each time point and a 95% confidence interval was calculated.

The remaining three lung segments were compared based on their lung sliding score and visual inspection of the ultrasound clip.

6. Results

6.1 Data collection

A total of 21 patients were included in this study. All patients were admitted to the ICU due to respiratory failure caused by SARS-COV-19 infection. A total of 477 DICOM files were created during this research. Demographic data are visualized in table 1. More men than women were admitted to the ICU and the women were older.

Number of patients	21	
Sex (m/v)	16/5	
Mean age (m/v) [std]	54 [12.5]/67 [6.8]	P = 0.04
Total recorded US images	477	
Modes (n=61):		
# CMV	18	
# ASV	26	
# Spontaneous	17	

Table 1: Table with demographic data

6.2 Characteristics and general performance of the FBST algorithm

The trackability of the FBST algorithm was tested on three ultrasonographic samples. Tracking the pleural movements was unreliable when using the FBST algorithm alone, which was indicated by the glitching movement of the tracking block. Tracking of intercostal muscles and diaphragm were remarkably better by eyeballing the number of glitches. An example of a representative glitch is depicted in figure 8.

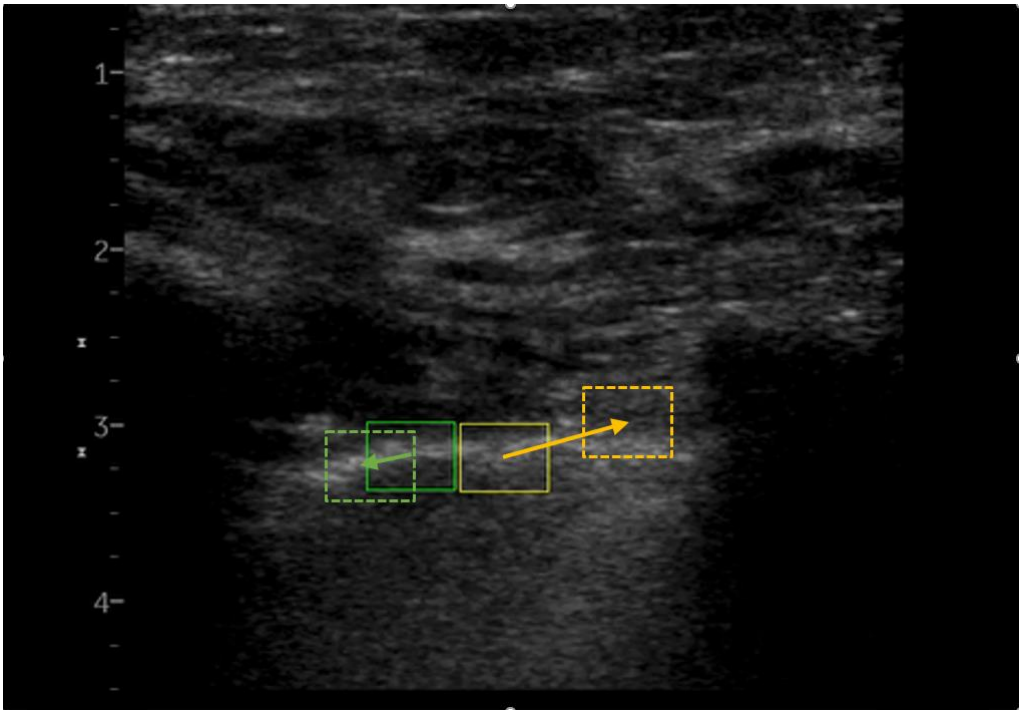

Figure 8: Example of glitch during lung sliding quantification. The solid square is the location of the speckle pattern in the current frame. Next location of the speckle pattern as the algorithm proposed

is indicated by the dotted square. Green tracking block displacement is in line with plausible translation. Yellow tracking block translocation is unplausible and called a glitch.

Upon closer examination of the probability map, it was ascertained that the algorithm is unfortunately unable to discern a correlation peak to the location where the speckle pattern has moved. We observed that the probability is almost equal across the entire pleural line. A 3D representation of the probability map is depicted in figure 9. Because the locations of the speckle patterns could not be followed in time due too low uncertainty, FBST was considered unusable for the application of lung sliding detection.

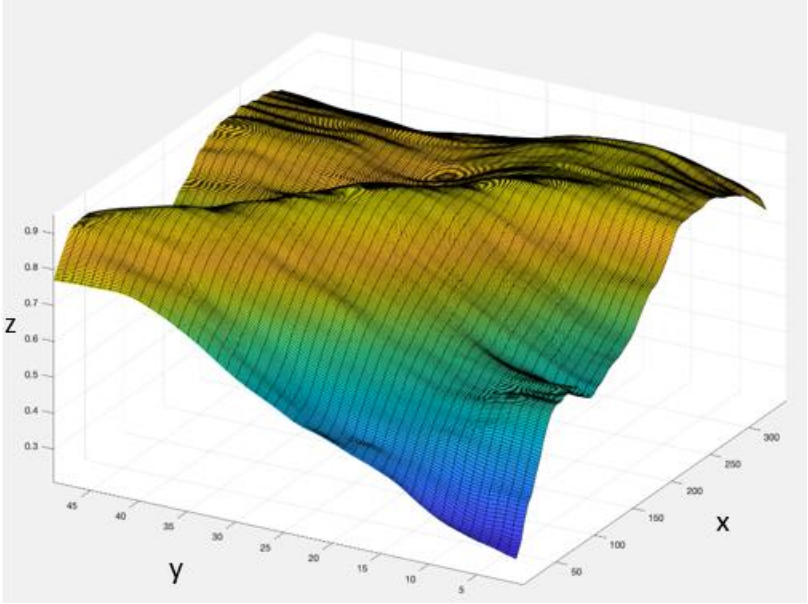

Figure 9: Probability surface of ST algorithm. The Z axis represents probability between [0..1]. One distinctive peak is missing in the surface.

6.3 Characteristics and general performance of the IBST algorithm

The IBST algorithm had an overall successful tracking rate of 88%. Most errors occurred due to incorrect initial pleural line detection and real-time segmentation of the pleural line by the Vesselness filter. This resulted in failure rates of 8.4% and 4.5%, respectively. A total overview of the different mistakes is depicted in table 2. Appendix A2 graphically show the typical mistakes made by the algorithm.

	N
Ultrasound examinations	477
Successful examinations	420
Initial pleura detection mistakes	
- A-line segmentation	18
- Muscles segmentation	19
Real-time pleura segmentation mistakes	20

Table 2: Overview of different mistakes that caused incorrect analysis of pleural movement.

An example of a pleural movement analysis signal using the IBST is depicted in figure 10. The respiratory phases can be differentiated by the two peaks in the IBST signal, the peaks are depicted with the blue and orange triangles. The inspiratory phase starts at the beginning of the peak with the

orange triangle. The expiratory phase starts in between the blue and orange peak where it makes a turn into an increase of lung sliding caused by the lung deflation.

A movement signal is combined with flow and pressure information of the ventilator. Figure 10 depicts an accurate delineation of the flow and lung movement, suggesting a correlation between lung movement and lung flow.

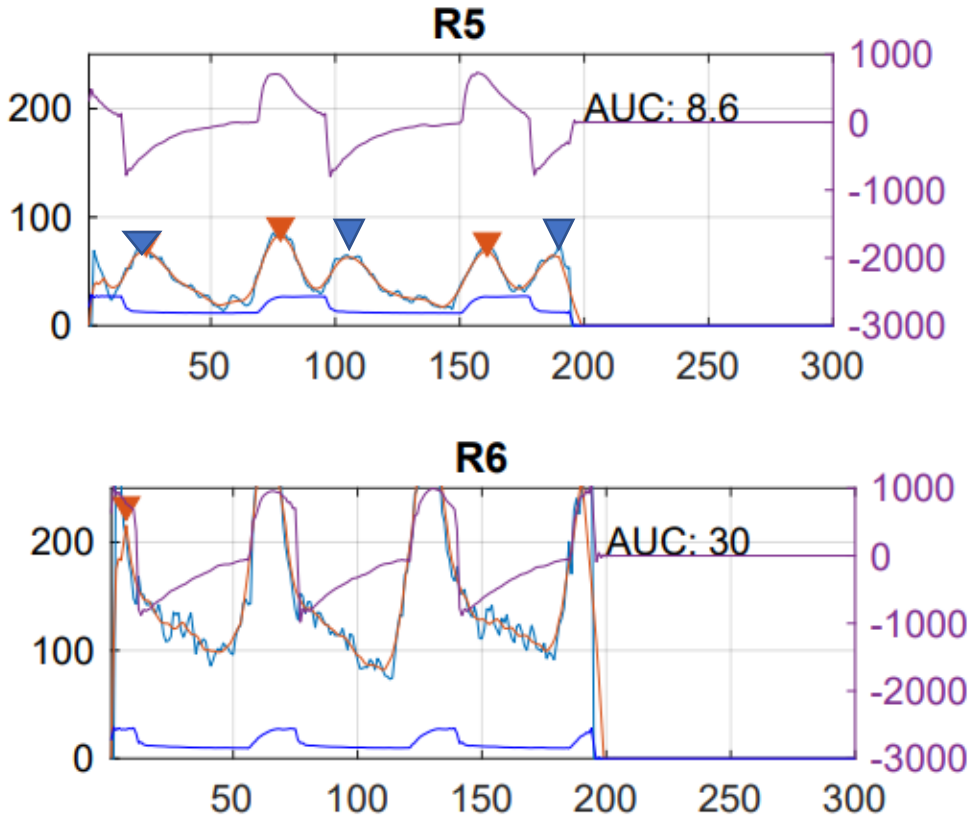

Figure 10: Two examples of IBST signals combined with flow and pressure data of the Hamilton C6 ventilator. Figures R5 and R6 show an increased signal together with the increase of flow. Figure R5 shows an increased IBST signal (blue triangle) together with an inverse flow. Note that the IBST signal resembles the absolute signal of flow. Purple line represent flow in [ml/s], light blue line represents raw IBST signal, orange line represent filtered IBST signal and dark blue represents pressure in [cm H20].

Comparing radiological images with the IBST movability score suggested that the IBST score is able to recognize pulmonary abnormalities. A representative example of this is depicted in figure 11 which shows that a lower score of IBST was observed right versus left in a COVID patient with predominantly right sides pulmonary abnormalities.

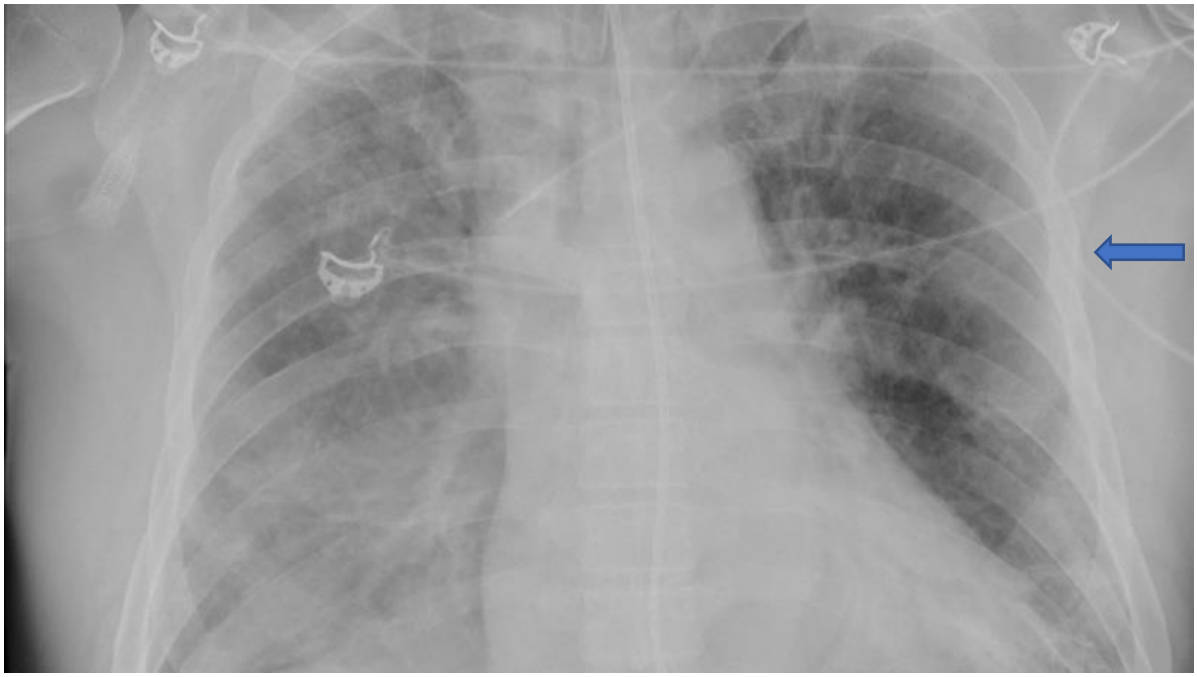

Figure 11: Radiographic thorax image of a COVID patient with pneumonitis and subsegmental pulmonary embolisms. Consolidations can be seen bilaterally, especially in the right lung. The corresponding mean IBST scores were 22.4 in the left lung and 15.3 in the right lung. The blue arrow pointed to the left lung is more aerated because more black on a radiological image represents more air.

6.4 Validation experiments

A: Expert lung sliding quantification versus lung sliding quantification algorithm

Interobserver agreement of the lung sliding assessment was 56%. The boxplot in figure 12 visualizes the correlation between the images categorized by the experts and the IBST score. The IBST score discriminates well between slight to moderate lung sliding and normal lung sliding as assessed by experts. As only one image was categorized as no lung sliding with a corresponding IBST score of 6.9, this category was merged with the moderate lung sliding group and the resulting category was renamed as slight to moderate lung sliding. The slight to moderate lung sliding group and the normal lung sliding group had a mean IBST score of 12.1 and 29, respectively. These groups were significantly different in IBST scores with a P-value of <0.001.

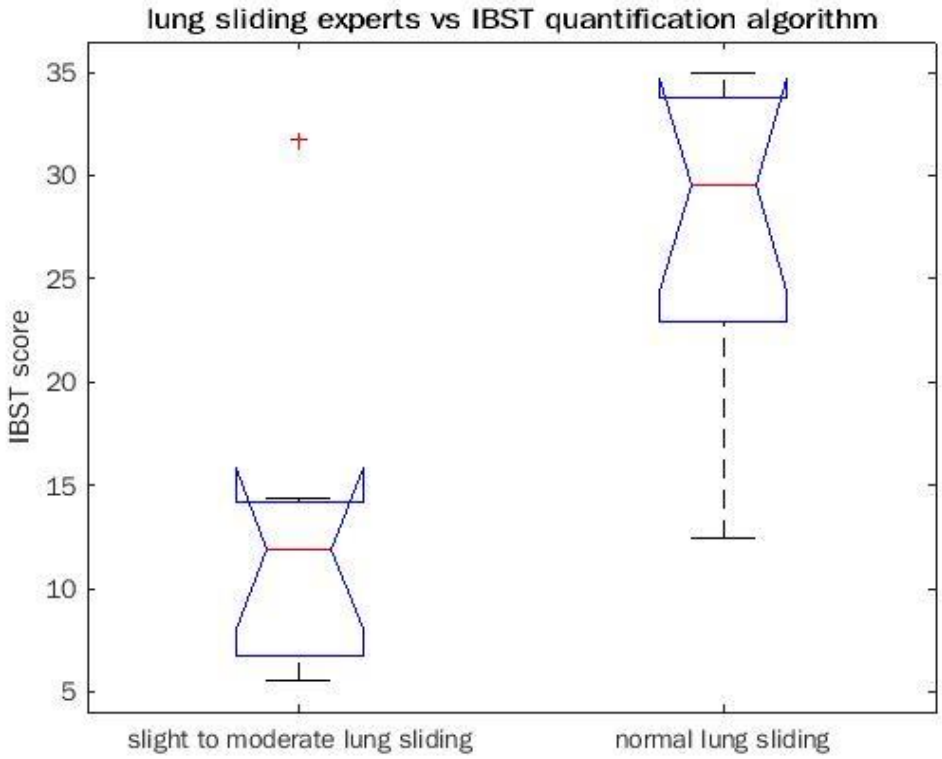

Figure 12: Boxplot describing the correlation between the categorization of lung sliding by medical experts and the IBST score. The normal lung sliding group (n=11) had a significantly higher IBST score than the slight to moderate lung sliding group (n=9). One outlier is marked with a red plus. The normal lung sliding group had an overall higher variation of IBST scores compared with the slight to moderate lung sliding group.

B: Correlation between IBST score and compliance

Data of ten patients in total were used to find a correlation between the IBST score and lung compliance. Two patients were measured twice and three patients were measured three times. Within patients with repeated measurements, we found an overall positive correlation between lung compliance and the IBST score averaged over all lung zones (figure 13). However, the slope and intercept between the patients differed. A linear mixed model corrected for repeated measurements was fitted between the individual points in the right scatterplot in figure 13. Lung compliance was associated with IBST score (β 0.15, SE 0.025, 95% CI 0.101-0.208, P <0.001).

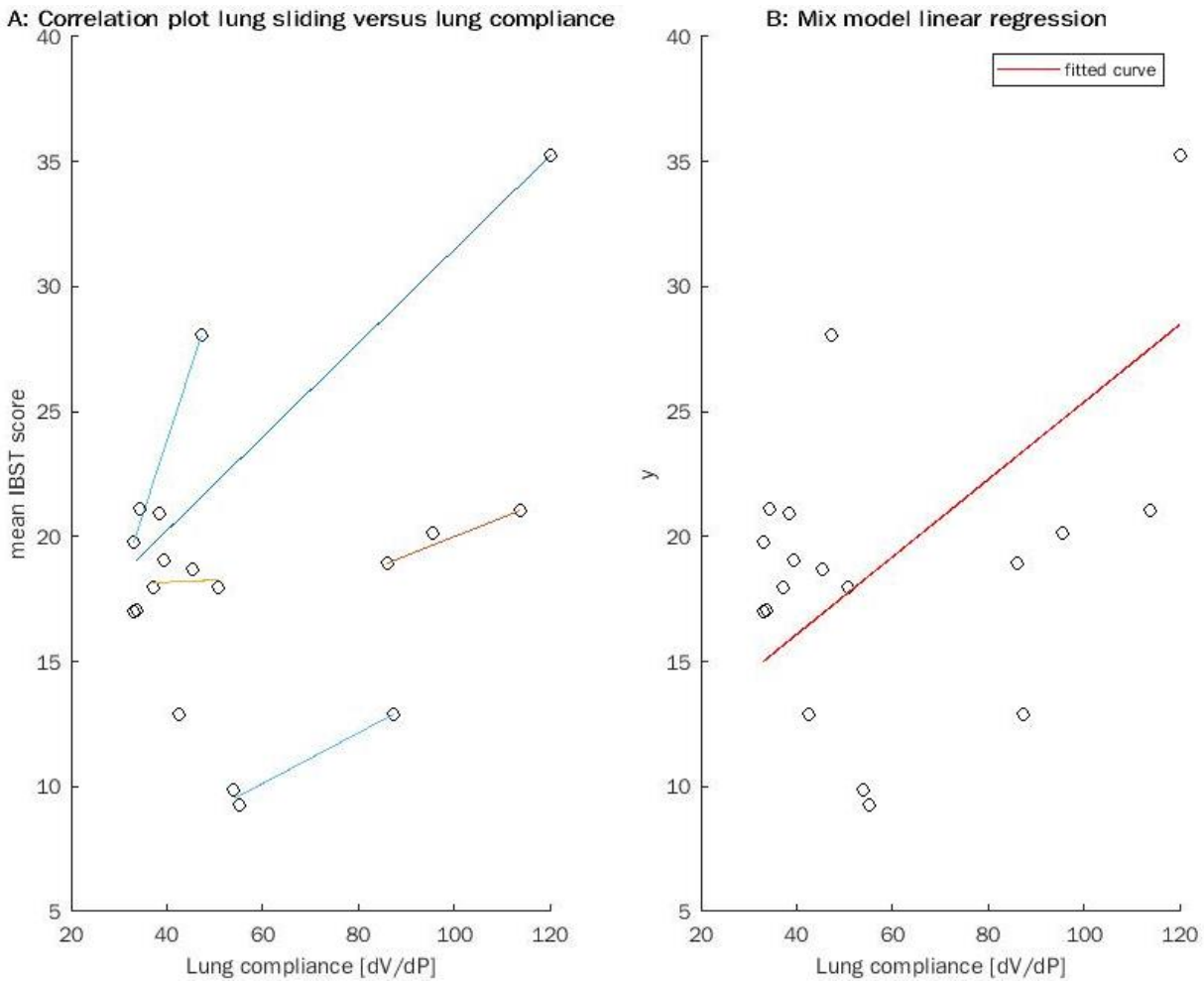

Figure 13: Scatterplot for the correlation between lung compliance and IBST score. Each colored line in the left scatterplot represents one patient. The red line in the right scatter plot represents the fitted linear mixed model.

C. Correlation between IBST score and overdistention

Patients were divided in two equal groups of n=9 based on PEEP value. In patients with PEEP below 12 cm H2O, the mean IBST score of the four frontal regions was significantly higher than in patients with PEEP equal or above 12 cm H2O with a mean ± SD of 20.9 ± 7 and 12.6 ± 6, $p < 0.05$ respectively (figure 14). Both groups were normally distributed. One outlier was detected with a mean IBST score of 23 and a PEEP of 16. No significant differences in age or lung compliance between the two PEEP groups were detected.

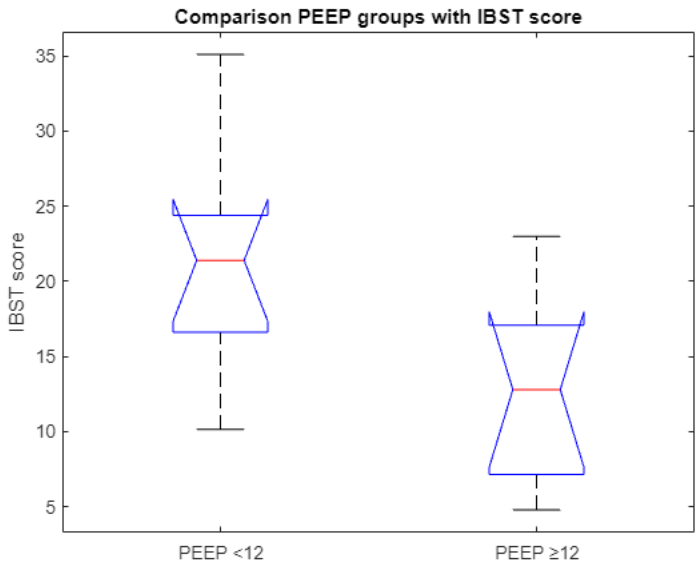

Figure 14: Boxplot describing the correlation between the PEEP groups and the IBST score. The PEEP <12 group (n=9) had a significantly higher IBST score than the PEEP ≥12 group (n=9).

6.5 Reproducibility of IBST algorithm

An example of the IBST signal of L6 with a 95% confidence interval is depicted in figure 15. Standard error of the IBST score in L6 was 2.7. The L5 and R6 measurement showed no reproducibility. The images of R5 consist of consolidated lung tissue and the IBST scores of these images were consistently low.

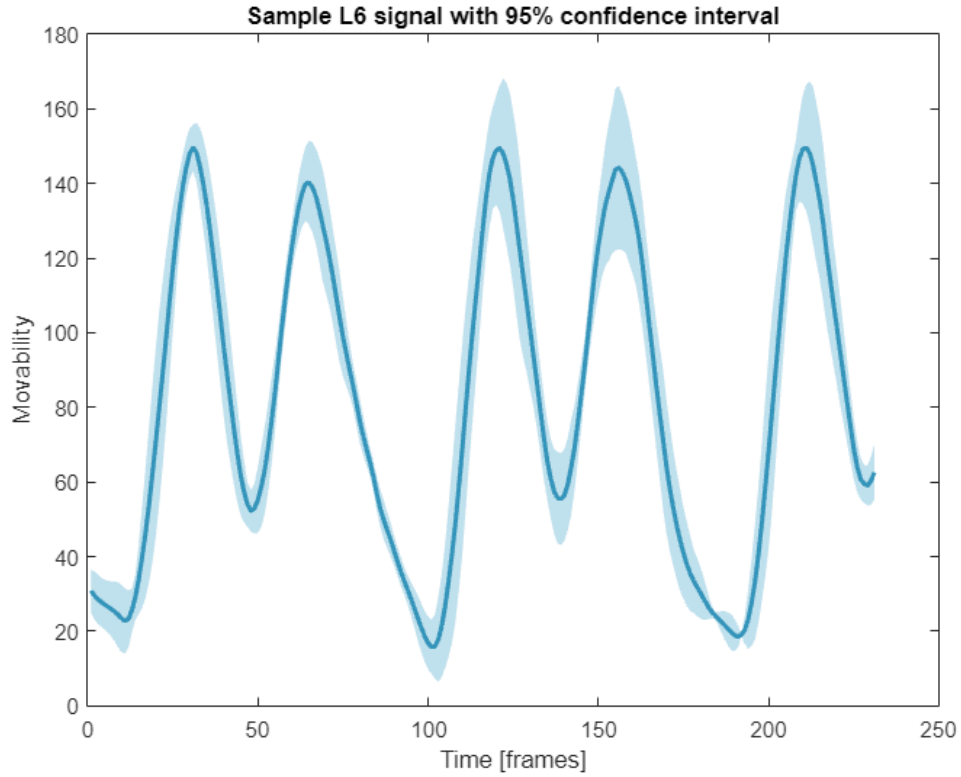

Figure 15: IBST signal of lung segment L6 with 95% confidence interval. The value of movability is dimensionless. Dark blue represents the mean between the repeated measurements and light blue represents the 95% confidence interval per sample time.

7. Discussion

7.1 Study findings

In the present study we explored the use of lung sliding quantification using the in-house made speckle tracking algorithms. Intensity-based speckle tracking (IBST) was a robust measurement for lung sliding quantification. Whereas, Fourier-based speckle tracking was not able for lung sliding quantification. Lung sliding quantification using IBST correlates well with lung compliance and lung sliding scoring determined by lung sonography experts. Our correlation with expert opinion showed strong evidence that the algorithm can score the level of lung sliding as good as the lung sonography experts. Considering the fact for high interobserver variability, this might suggest that the algorithm could potentially score the lung sliding even better than lung sonography experts.

To our knowledge, this study also shows for the first time that lung sliding quantification is feasible to detect lung overdistention. Therefore, lung sliding quantification can potentially be used for lung overdistention monitoring. This can be inferred by the observation that a decreased lung sliding is correlated to a decline in lung compliance at the final stage of inspiration in frontal regions. According to our data, a significant decline in mean IBST score between frontal regions in the patient group (>12 PEEP) compared to patient group (<12 PEEP) suggests that lung ultrasound monitoring could detect lung overdistention. This difference could not be indicated by a PEEP threshold alone, so further regional measurements will be needed for confirmation. To do this CT or EIT imaging methods serve as the standard for identifying overdistention. However, CT scan based evaluation of lung overdistention is rarely utilized in a non-research setting due to the labor-intensity of transportation of patients as well as radiation exposure. Unfortunately, EIT is not available in our hospital but may be accrued for follow up experiments.

7.2 Intensity-Based Speckle Tracking

IBST uses speckle intensity changes to measure lung sliding. The algorithm works better than the FBST algorithm because the speckle pattern does not need unique speckle patterns to track. Using IBST, speckle alteration is followed at a static location and is termed as speckle tracking decorrelation (SDC). (20). However, a disadvantage of the speckle tracking decorrelation method is difficulty distinguishing sonography plane directionality. For the application of lung sliding quantification, the direction of the lung movement is not relevant or realized using ventilator data. As such, SDC is already used to quantify blood flow in ultrasonic applications but not yet used for lung sliding quantification (20).

The IBST output is a clear recognizable signal that is conform the ventilator data. Both the inspiratory and expiratory phases can be differentiated. Also, the I:E ratio which is presented as the proportion of the inspiratory and expiratory phases in one breath cycle was visually recognizable in the IBST signal. Furthermore, the IBST output score was compared with a radiological image. There was a clear visible difference in aeration caused by a predominantly right sides pulmonary abnormality. The IBST showed the same difference in IBST score between both sides, suggesting that the less aerated lung has less lung sliding. The morphology of the IBST signal may contain also information on lung pathologies. Auto PEEP for example could delay the lung deflation resulting in a lower expiratory peak and a decrease in the IBST signal. However, these effects were not investigated in this study.

Overall, the segmentation performance of the algorithm was not bad, with a segmentation failure rate of initial pleura line detection and real-time segmentation of 8.4% and 4.5%, respectively. Because of the significant change of inaccurate measurements, each image must be checked manually. Segmentation of the pleura was based on intensity thresholding and morphological operations and is a simple method to segment the pleural line. More robust methods for pleural line detection are random walk algorithm (21), Radon transform line detection (22), and neural networks-based segmentations (23) and could increase the performance of the IBST algorithm (24).

Several articles describe lung sliding quantification for pneumothorax detection, but none mention the effects of lung compliance and overdistention on the lung sliding quantification. Duclos et al. and

Lichtenstein et al. both suggest that lung sliding quantification could be used to detect alveolar stress (10, 25). We validated the IBST algorithm score against lung compliance and found a positive correlation. Together with our observations, and lower IBST values in overdistention sensitive areas, we agree that lung sliding quantification could be a tool to detect lung overdistention.

7.3 Validation experiments

The automatic quantification of lung sliding cannot be validated using a golden standard. A previously performed literature study found no comparable lung movement algorithm that could be used to benchmark the algorithm (appendix A1). The lung ultrasound (LUS) score is an accepted method for evaluation; however, this score is mainly based on lung aeration and not solely on lung movement. (25) Lung sliding is only evaluated as existing or none-existing, so scoring is unable to represent the gradation of lung sliding.

Therefore, the movability of the lung sliding was assessed by ultrasonography experts. High interobserver variability was observed in the study between the subjective scores of lung sonography experts, which could be due to missing scoring criteria. A clear correlation was found between the IBST score and the experts' opinions. Thus, the algorithm is performing as proposed. The data consists of one outlier. This might be caused by a fast-changing pleural movement with limited displacement, or interpreted wrongly by the sonography experts. Present research showed for the first time a comparison between a subjective gradation of lung sliding and a quantitative gradation of lung sliding.

Besides movability validation, lung compliance was compared against the outcome of the IBST algorithm. Lung compliance was chosen because long movement is proportional to lung compliance, and the increment of lung volume cause lung expansion and, therefore, lung movement. Regional compliance is normally not validated against the lung compliance measured by the ventilator. EIT is also able to measure regional compliance and was validated using CT (26), electron beam computed tomography (27), and positron emission tomography (28). Due to time and budget constraints, we couldn't validate our results with those measurements. We proposed that the average IBST scores between the LUS regions should follow the same directions in correlation with the lung compliance and give a rough estimation of the performance of the IBST algorithm. The IBST score and lung compliance are positively correlated. However, these correlations can only be determined within the same patient because anatomical differences, such as BMI, length, and sex, could influence depth and size of the lung.

Furthermore, we tested the correction by averaging all lung regions with a maximum of 25% missing data. Even with missing data the data was significantly correlated with lung compliance measured globally from the ventilator. The effect of lung compliance on the IBST score appears to be strong despite the considerable wide CI and variation between patients. This evidence suggests that IBST might be more feasible to measure regional lung compliance. However, this needs further investigation.

Finally, we investigated if the lung sliding quantification algorithm could be used for the prediction of lung overdistention. The data presents, a significant lower IBST signal in patient ventilated with a PEEP of twelve or above. These patient were more prone to lung overdistention in the frontal regions than patients ventilated with lower PEEP pressures. The hypotheses of lung sliding reduction by lung overdistention seems therefore reasonable. Some outliers show a high IBST despite ventilated with a high PEEP. This might indicate varying PEEP thresholds for lung overdistention among patients. So further regional measurements will be needed to further investigate the IBST threshold for lung overdistention.

7.4 Reproducibility

Three repetitive measurements used on the same lung segment were compared and variation was discovered. Fluctuation in the measurements causes low reproducibility on the IBST score. This was indicated by varying pleural line depths between the three measurements. We suggested three possible causes: incorrect reposition of the ultrasound probe, unequal pressure applied to the ultrasound probe, and alternating angles of the ultrasound probe. However, for monitoring purposes, an ultrasound sensor applied with a biocompatible adhesive should countervails the incorrect position, varying pressures, and angles of the ultrasound sensor.

Further problems include speckle bleaching, incorrect segmentations, and ultrasound interference. First, bleaching occurs when the gain setting of the ultrasound is set too high, and no changes in intensities can be observed. Thus, gain adjustments affect the IBST score, and the author suggests keeping the gain at a minimum. The pleural is a high echoic line, so a low gain poses no interference. Second, fluctuations in IBST score were caused by partial segmentation of pleural tissue below the rib, resulting in underestimated movement quantification. Segmentation errors can be solved by optimizing the segmentation strategy by using more advanced segmentation algorithms. However, more advanced programs necessitate additional computational power, such as cloud computation, when developing low-cost sensors. Ultrasound interference can occur when more ultrasound beams are transmitted simultaneously. This could be problematic for lung sliding sensor usage on the same patient. Third, interference problems can be overcome by repetitive imaging of the lungs in combination with time synchronization between the sensors.

7.5 Fourier-Based Speckle Tracking

Two articles also described effective implementation of lung sliding measurement for detecting the presence of a pneumothorax using GE Echopac software (10, 29). This software using pleural strain calculation is comparable with our in-house developed Fourier-Based Speckle Tracking (FBST) algorithm. However, the performance of the latter was significantly worse than indicated in the suggested articles. Multiple problems could cause this discrepancy. First, the FBST algorithm currently works with the DICOM data format. The focus of DICOM data was mainly due to the inaccessibility of the RF data and the easy direct export of DICOM data from the Lumify tablets. The conversion of RF data to DICOM data consists of speckle filtering operations; therefore, the tracking block has trouble finding the exact speckle composition in the image. Second, the frame rate of 30 fps might be too low to find moving speckles. Speckles move in three-dimensional space, and in between two frames, the speckles could move out of the two-dimensional plane of the ultrasound image. Third, the GE Echopac software uses an unknown number of tracking blocks, whereas our algorithm uses two tracking blocks. If the GE Echopac software used more tracking blocks, the algorithm might be less sensitive to errors caused by one misplaced block since strain values are averaged over the targeted tissue. This is outside our knowledge and averaging multiple tracking block are not yet implemented in the FBST algorithm. Our findings with speckle tracking pleural movements are consistent with the finding of Rubin et al. who used SP to track lung motion for radiotherapy (30) and concluded that that difficult tracking of the pleural line is due to the presence of specular reflections instead of the standard speckle source composed of distributed speckles. Thus, RF data and frequency filters were needed to gain sufficient tracking results.

Besides technical limitations, there were anatomical limitations. First, the pleura of the lung is a thin structure, causing insufficient size of speckle compositions and therefore difficult to track. In contrast, speckle tracking in the heart works well due to thicker muscle walls, creating better quality speckle patterns. Secondly, speckle movement occurring parallel to the transducer facilitates more favorable results than perpendicular movement occurring during lung sliding (12,13). Unfortunately, performing ultrasound in another direction is very difficult. Thus, lung sliding still remain difficult to track.

7.6 Limitations

Most of the correlations identified in this thesis were based on a small database of patient information. No power analyses were performed before the data collection started. A second limitation was caused by the uncorrelated speckle method. The measurement of movability is not yet calibrated against a lung sliding phantom model. We also do not know if the movability score increases linearly with the duration and velocity of pleural movement. Besides, a maximum limit in movement detection is dependent on the framerate setting of the ultrasound transducer. Third, our patient population includes only COVID-19 patients, and no comparison was identified with healthy volunteers. Lastly, data acquisition was performed by only one, inexperienced sonographer; therefore, data may be skewed.

7.7 Future research and perspectives

Additional research is required to further improve the IBST algorithm for lung sliding quantification, and a ready-to-use program needs to be developed for easy application. Presently, the IBST score only indicates a score on the movability of lung sliding. however, an IBST threshold needs to be validated using EIT or CT scans for detecting overdistention. Furthermore follow up studies should investigate the effects of incorrect positioning, pressure, and angle of the ultrasound sensor on the variability of the IBST score. It may also be beneficial to discover if the algorithm could be used for the diaphragm and intercoastal muscle tracking, as diaphragmatic function is a proven predictor of a weaning outcome but the use of it is hampered by the fact that automatic detection and continuous quantification of this is as of yet not possible (23). Since, ultrasonography may provide an anatomical view, whereas for example EIT only provides an electric signal. Additional diagnostic information can be extracted using a gray-level co-occurrence matrix analysis, providing better diagnostic accuracy in differentiating cardiogenic pulmonary edema (CPE) and ARDS (31). Future studies should focus on the delivery of continuous imaging of the lung using ultrasound which may provide relevant clinical information.

If multiple indications such as lung sliding, diaphragmatic function and automatic continuous B-line detection to screen for fluid overload may be combines a wearable ultrasound solution could be used as a multipurpose measurement device. Taken together we feel that this project paves the way for several follow up projects aiming at providing the clinician with real time information on regional abnormalities, overdistention, fluid overload and diaphragmatic function.

8. Conclusion

Two lung sliding algorithm were developed to quantified lung sliding. Intensity-based speckle tracking (IBST) was a robust measurement for lung sliding quantification. Whereas, Fourier-based speckle tracking was unable for lung sliding quantification. IBST scores correlates well with expert opinion and lung compliance, but the reliability needs improvement. Moreover, this study suggests that lung overdistention results in a reduction of lung sliding and implementation of this method may improve detection of overdistension. Additional research is needed to further validate the algorithm score and the potential impact on clinical detection as well as the optimization of mechanical ventilation.

A1. Literature Review

The current state of lung measurements during ventilation in the intensive care and the possibilities of continuous ultrasound lung monitoring. A literature review.

J.M. Visser[a]

[a] *MSc Student Technical Medicine, Delft University of Technology, Delft; Erasmus Medical Center, Rotterdam & Leiden University Medical Center, Leiden; The Netherlands.*

Abstract

Patients ventilated in critical care units may suffer from iatrogenic ventilator-induced lung injury (VILI). VILI is the result of volutrauma and barotrauma on the lung as a result of mechanical ventilation. Furthermore, the lungs may be overloaded by fluids during ICU treatment which may also severely impact the lungs and increase needed mechanical ventilation pressures. Although many proposed techniques have been suggested to minimize VILI, we aimed to provide an overview of diagnostic methods that may be able to help us in optimizing mechanical ventilation in such a way that VILI may be prevented. Upon review of the literature, we have identified several studies that have investigated the methods that may be used to prevent VILI. With this aim, we reviewed these methods and focused specifically on methods that may be used to prevent VILI and/or fluid overload in the lung. We found that trans pleural pressure measurements may be helpful but cannot accurately approximate regional overdistension due to an uneven distribution of air delivery in different regions of the lung. Electrical Impedance Tomography (EIT) can measure regional- air distribution, lung overdistention, and lung collapse, but the use of this method is hampered by financial and logistical reasons. Ultrasound is mainly of use to screen for fluid overload and may be used to diagnose specific areas in the lung that have collapsed but is, as of now, not useful in optimizing ventilator settings to prevent VILI. Taken together, in this literature review, we show that EIT and ultrasound may be helpful in specific clinical questions and may help us to personalize mechanical ventilation in the critically ill with regard to mechanical ventilation settings (EIT) and fluid overload (ultrasonography). However, we believe that ultrasound techniques may be developed that do help us in this regard. These techniques will be discussed in the thesis since literature for the use of ultrasound for these indications is lacking. The use of ultrasound to personalize ventilation is the main part of my thesis, and we believe that our focus on the utilization of ultrasonography as a more cost-effective and safer alternative for measuring alveolar stress and extravascular lung water levels may open new pathways for diagnosis and treatment.

Introduction

Intensive care patients generally present with respiratory and circulatory insufficiencies. Intensivists and the diagnostic team seek to monitor and support these systems with minimal and iatrogenic damage. Patients diagnosed with acute respiratory distress syndrome (ARDS) or other diseases, such as COVID-19 suffer from lung abnormalities. The result of the abnormalities is that an uneven air distribution within the lungs develops, which causes a higher-pressure load in the relatively unaffected lung parts [1]. This phenomenon is also known as the "baby lung" which stands for a relatively unaffected area of the lung without regional lung edema and atelectasis. Mechanical ventilation is supposed to open and ventilate the closed lung parts but at the same time minimally affect the relatively healthy "baby lung". The damage to the lungs is induced by high-pressure ventilation (barotrauma), over-extension of the lungs (volume trauma), and re-collapsing alveoli (cyclic atelectasis). Thus, VILI can occur in any lung disease but most frequently in ARDS. The damage progressively increases over time when the lung is mechanically ventilated [2]. Research has shown that the protective ventilation strategy is associated with a higher survival rate for critical patients (28 days) [3]. For successful protective ventilation, the tidal volumes must be sustained below 6 mL/kg, not exceeding a plateau pressure of 30 cm H20 to prevent volume trauma. To

minimize small airways from collapsing, optimization of the Positive End-Expiratory Pressure (PEEP) will contribute to sustained recruit ability, lung homogeneity improvement, and an increased total aerated lung volume [2, 4]. Frequently, optimizing the PEEP settings can reduce barotrauma by decreasing the potential for too high PEEP values and preventing collapsed airways due to too low PEEP values.

In addition to ventilation, patients are frequently filled with fluid to support their hemodynamic system. However, the fluid needs to be extracted at a certain point due to overload, causing edema and vital organ failures [5]. Clinical studies suggest that a negative fluid balance can reduce time on mechanical ventilation and even reduce mortality [6]. Monitoring the presence of fluid inside the lungs can optimize the patient fluid balance and is key to the surveillance of patients with subsequent cardiac problems.

Several medical devices have been created which are able to monitor pulmonary congestion and alveolar stress, but technological innovations are still needed to further address the ventilation and pulmonary congestion problems. Most of the lung monitoring devices as of present are invasive or introduce radiation; however, new research shows that non-invasive techniques, like ultrasonography, can monitor the lung similar to other conventional measurements. Thus, ultrasound devices are still being developed, and improvements have enabled the device to provide continuous data due to a micromachined ultrasonic transducer.

We aim in this literature study to review clinical studies that evaluate lung monitoring devices used in intensive care to support mechanical ventilation. Secondly, we investigate if ultrasound can be an alternative to those measurements. Finally, we aim to investigate if continuous ultrasound is used in the ICU and what the potential for continuous ultrasound can be in the critical care environment.

Methods

Search

Relevant studies were found utilizing the Medline electronic database. The search terms are listed in Appendix A. The eligibility of the studies was evaluated by reading the title and abstract. Inclusion criteria are listed in the selection of articles section. All the articles were then sorted based on the measuring technique in a citation manager program (Endnote X9). Articles that were included were fully read and evaluated by the author.

Selection of articles

Articles were included if the following inclusion criteria were met:

- The article describes a medical device that is used to monitor the lung during mechanical ventilation.
- The article describes the measuring device as the main subject.
- The method is performed in adult humans.
- The article describes a (randomized) clinical trail.
- Patients mechanically ventilated in an intensive care setting.
- The article was published after 31 December 2009.

Results

Selection of articles

The final search took place on August 15, 2021, and resulted in 463 articles for selection analysis. After all exclusions, 74 articles remained for further assessment and were finally included. In total, five different measuring methods were found, as depicted in figure 1. Four articles regarding trans-pulmonary pressure, twenty-two articles regarding extravascular lung water (EVLW), sixteen articles regarding electrical impedance tomography (EIT), thirty-two articles regarding ultrasound (US), and zero articles regarding continuous ultrasound were found.

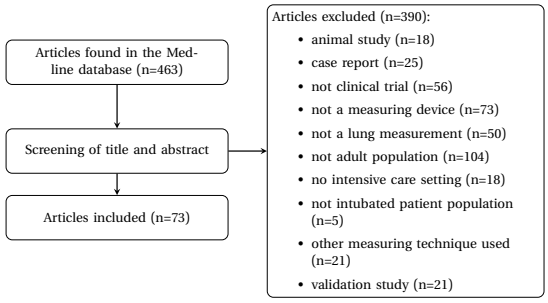

Figure 1: Flowchart describing the final search and exclusions of articles

Transpleural Pressure Measurement

A minimum PEEP pressure is needed to keep all of the alveoli open and is measured by the sum of the transpulmonary pressure and the transthoracic pressure. However, the ventilator has no way of differentiating between these two pressures. One method that seeks to measure and subsequently optimize transpulmonary pressures is the esophageal pressure

catheter. In transesophageal pressure measurement, a balloon catheter is positioned in the midthoracic esophagus, which is able to measure pressure and may be used to estimate the trans pleural pressure [7]. However, a disadvantage of this method is that it is assumed that the pleural space is a totally homogeneous volume, which is not the case. Trans pleural pressure as such can be useful to optimize protective mechanical ventilation since an "optimal PEEP" may be set, preventing unnecessary stress on the lung parenchyma and prevent VILI [8].

Research has described the use of transpulmonary pressures in ARDS patients to optimize titration of PEEP settings. Fiedler, et al. observed a strong correlation between end-expiratory lung volume and transpulmonary pressures that could potentially lead to a more individualized approach of titrating the correct PEEP for critical patients instead of targeted saturation [9]. However, Beitler, et al. investigated in a randomized controlled trial that transpulmonary pressure-guided PEEP compared with fi02 guided PEEP resulted in no significant difference in both ventilation days and mortality [10, 11]. On the other hand, another study describes data collected from a trial utilizing transpulmonary pressures guidance in Venovenous Extracorporeal Membrane Oxygenation (VV-ECMO), yielding an increase in ARDS patients successfully weaned compared to that of the control group (intervention yielding a 0-5cm H2O range) [12]. Taken together, although the use of transpulmonary pressures in mechanical ventilation optimization has great potential, the state of the art of evidence with regard to clinical endpoints is still ambivalent.

Extravascular Lung Water Measurement

Until recently, quantification of EVLW was not possible, as measurements were previously based on chest radiography and arterial blood gas analyses [13]. Subsequently, a single transpulmonary thermal dilution indicator was developed to detect small increments of EVLW measurements, ranging between 10-20% [14]. The thermal dilution curve is used to calculate the intrathoracic thermal volume as well as the total pulmonary volume, contributing to the effective calculation of the EVLW measurement [15]. Although this technique indicates small measurements, it is invasive and expensive [15].

Previous studies describe a positive correlation between EVLW or the pulmonary vascular permeability index (PVPI) and the severity of ARDS. The studies included the transpulmonary thermal dilution to measure EVLW. [16–24]. With respect to COVID-19 patients, higher EVLW measurements were observed as correlated to non-COVID-19 patients [23–25]. Also, a positive correlation was found between EVLW measurements and mortality [18–20, 26–29]. Alternative methods that were studied use EVLW to monitor: Fluid management [30], hemodialysis [31, 32], peep titration [33], pleural effusion [34], recruitment manoeuvre [35, 36], sepsis survival [27, 28] and weaning [37].

Electrical Impendance Tomography

To prevent VILI, we need to set the mechanical ventilator in the most optimal way. Incorrect settings cause high transpulmonary pressures, alveolar overdistention, cyclic recruitment/de-recruitment, and biotrauma [38]. In acute lung injury, it is desired to optimize ventilation based on the quantity and location of lung atelectasis and pulmonary edema. However, because measuring regional ventilation distribution is clinically challenging to assess, a computed tomography (CT) scan can be used to assess the aeration of the lung. Although this is an effective method to use, it is not suitable for investigation at the bedside nor for extracting dynamic information. Another technique, EIT, utilizes multiple electrodes around the thorax to measure the lung tissue dielectric properties with movement. Overdistention can then be determined by the end-expiration air volume minus the tidal variation [38]. Due to the novelty of this technique, further studies are needed, and the cost-effectiveness of its integration in clinical settings would need to drastically increase.

EIT measurements may be used to set optimal PEEP and doing so has been evidenced to affect and aid in especially lung recruitment and overdistension [39–49]. Six studies of which used EIT to examine the optimal PEEP setting [39, 41, 42, 44, 46, 48]. Four studies investigated the effect of lung recruitment and showed that EIT is able to identify correct lung recruitment [45–47, 50]. Two studies used EIT to measure the percentages of lung overdistention [41, 51].

Three additional studies evaluated the effects of posture therapy on regional ventilation distribution using EIT and showed that a prone versus supine postural position had a positive effect on tidal volume distribution [52]. In terms of regional tidal volume distribution, a lateral versus supine postural position did not induce a significant change [53]. Conversely, targeted lateral positioning in mechanically ventilated COVID-19 patients indicated a decreased lung collapse as well as lung overdistension [48]. One such

study investigated the use of EIT to estimate global lung strain and compared it to the golden standard CT and was positively and independently associated with EIT measures [54].

Ultrasonography

Besides invasive techniques, non-invasive echographic examination of the lung using B-line scoring can also be used to evaluate EVLW values and alveolar stress. The numbers of comet-tail tracers and lung pleural morphology in twelve zones around the thorax can be used to calculate the lung ultrasound score (LUS) [55–69]. With respect to B-line scoring, this method is correlated with effective thermodilution method compatibility and has higher accuracy in EVLW detection and also in comparison with chest radiography [55, 62, 65, 68, 70]. To further investigate the effects of daily B-line scoring on fluid management, Rasu, et al. found no significant difference in cumulative fluid balance and mortality [67]. Several studies evaluating the use of ultrasound to monitor for fluid overload are, however, still ongoing. It is conceivable that more frequent or continuous monitoring may reduce fluid overload and improve clinical outcomes. However, in certain settings, lung ultrasound may be better than EIT since EVLW traceability may be negatively impacted by inflammatory interactions, which impact overall measurements and reliability [66, 71].

Two studies investigated the optimization of PEEP settings when the LUS was used. These studies indicated that PEEP lung recruitment could be guided and monitored using ultrasonography. Controversially, they discovered that lung hyperinflation could not be assessed solely by means of LUS [58, 72].

It is possible to use the data derived by LUS to make a diagnostic analysis using an algorithm that analyzes the gray-level co-occurrence matrix of the lung yielding reliable data for differentiating between cardiogenic pulmonary edema (CPE) and ARDS [73].

Another possible ultrasound application to measure alveolar stress is to quantify the amount of lung sliding, which is a dynamic hyperechoic line that indicates the effects of the movement of the visceral pleurae against the parietal pleurae during respiration [74–76]. Quantification of the pleural movement was analyzed using speckle tracking technology developed initially to quantify cardiac strain [77]. Speckle tracking uses convolution with a particular pattern followed in the time domain and can measure the displacement (mm), the direction, and the velocity. Results from lung sliding quantification speckle tracking evidenced positive results for further classification of pneumothorax versus non-pneumothorax patients [74]. Additional research was regarding LUS and lung aeration correlation in COVID-19 and discovered additional monitoring techniques benefited the diagnostic process [78–81]. finally, LUS monitoring uses were particularly helpful in these areas: Acute chest monitoring [82], diaphragm atrophy monitoring [83], ECMO monitoring [84], lung lesion monitoring[78], poisoning monitoring [85] and neuro care. [57, 64]. We believe that pleural lung sliding may be used to measure alveolar stress, which may help us in understanding the stress in different areas of the lung and optimize mechanical ventilation. This is the main subject of my thesis. We have found no relevant literature on this topic so far.

Continuous Ultrasonography

Since previous studies have shown that ultrasound may be helpful in restricting fluid overload to the lung as well as aid in optimal mechanical ventilation settings, we have searched for studies that have investigated continuous ultrasound to these effects. However, to the best of our knowledge, no such studies as of yet exist. It is however, an interesting area to develop. Conventional ultrasound probes consist of multiple rows of approximately 120 piezoelectric crystals, separately wired to the connectors via a heavily protected probe. Although ultrasound semiconductors do not utilize crystals such as these, capacitive zone integrated on a silicon chip transduce signals for receiving and transmitting sound waves. The sensors, wires, and electrical circuits, manufactured through thin film photolithography, can be placed on the same chip making it very thin and cost-effective for mass production. Another advantage of this method is the preprocessing ability of the integrated computational circuit, in which raw data may in the future be converted into digital imaging. This structural difference contributes to more efficient communication and usage due to fewer wires and less data interference. Due to the small form factor of the chip and special ultrasound gel, the ultrasound sensors can be attached to the human body for more than 48 hours, making it great for continuous monitoring. Moreover, the sensors are small and inexpensive, so in clinical practice, we could attach more than one sensor to monitor different locations in real-time. As such, because there are no present clinical studies that have addressed continuous ultrasonography integration, this provides an avenue for future research.

Discussion

Currently, the prevention of VILI is an important topic in critical care, as effective techniques are always being analyzed for implementation. For example, esophageal pressure measurements represent changes in pleural pressure, and values such as these contribute to viable implementation of techniques that prevent VILI potentiality. However, this technique cannot give a good approximation of regional overdistension due to the uneven distribution of air delivery in ARDS patients. Due to the uneven distribution that is unique to every single patient, a more personalized approach to ventilation could be a solution to prevent VILI. A study by Constantin et al. investigates the effect of personalized ventilation on the survival of ARDS patients compared with standard care patients [86]. In this particular study, patients were divided into a focal and a non-focal ARDS group, each with a different treatment strategy using low and high PEEP, respectively. The morphology of the lungs was determined using a CT scan. The authors found a survival improvement using personalized ventilation. Nevertheless, the study found that wrong determination of lung morphology (focal versus non-focal) could harm the patient significantly, and implementation should be carefully considered [86]. As such, correct classification of lung morphology is an essential step when using personalized ventilation care.

With respect to lung morphology in ARDS patients, monitoring is seen to progressively change over time due in part to personalized ventilation settings. Upon analysis of techniques, it was observed that 1). A CT scan is unsuitable because of the unavailability at the bedside, radiation exposure, and costs 2). An EIT can be used but has some limitations due to its development status, high cost, and availability 3). Ultrasonography is more accessible and can monitor lung aeration changes as well. Subsequently, new developments are being analyzed for continuous monitoring through continuous ultrasound, but this area is still underdeveloped.

Besides VILI, fluid overload is another important theme in intensive care medicine. Invasive techniques such as a transpulmonary thermal indicator can be used to quantify fluid overfilling in the lung. This technique is relatively expensive and has possible side effects. Ultrasonography could be used to monitor both alveolar stress as well as lung fluid levels simultaneously. These values are able to be performed based on quantification of lung sliding and B line detection, specifically extracted from the same 2D post-processing image process. Thus, a combination of lung sliding and lung fluid information might also help develop an algorithm to determine correct ventilator settings. An overview of the pros and cons of the different measurements are depicted in figure 2

Our ultimate goal is to integrate lung monitoring solutions in combination with the ventilator. The idea is to integrate multiple transducers to specify information locally during lung ventilation. Monitoring devices such as continuous ultrasound can provide information on fluid overload in the lung and may in the future guide us in understanding lung overdistention. A model with these measurements could provide a closed-loop ventilator algorithm that regularly evaluates the ventilator settings and automatically optimizes the ventilation strategy.

Conclusion

In summary, this literature review provides an overview of multiple lung measurements and techniques that could improve ventilation strategy in critically ill patients. Every technique yields benefits as well as disadvantages, but alternative methods should be considered for cost, safety, and availability considerations. As such, ultrasonography may be an attractive alternative due to its accessibility and safety, but replacement techniques still need to be confirmed by non-inferiority studies. Future research may be dedicated to confirming ultrasound-guided monitoring of lung aeration and overdistension and could be used for guiding ventilation in healthcare settings.

Figure 2: Overview of measurements

Overview of measurements

1. Transpulmonary pressure

+ Etimation of transpleural pressure
− Effectiveness of new therapeutic strategy uncertain
− Invasive medical device

2. Extravascular lung water

+ Accurate quantification of extravascular lung water
− Invasive medical device
− Expensive

3. EIT

+ Quantification of regional air distribution
+ Measure lung strain and lung overdistention
+ Can optimize PEEP settings
− Expensive and low availability

4. Ultrasound

+ Non-invasive
+ Quantification of lung water
+ Quantification of alveolar stress
+ Could discriminate CPE and ARDS.
+ High availability

5. Continuous Ultrasound

+ Useful for long time monitoring
+ Measure trends
− Less image quality
− Less scientific research

References

[1] P. Radermacher, S. M. Maggiore, and A. Mercat. "Fifty Years of Research in ARDS. Gas Exchange in Acute Respiratory Distress Syndrome". In: *Am J Respir Crit Care Med* 196.8 (2017), pp. 964–984. ISSN: 1535-4970 (Electronic) 1073-449X (Linking). DOI: 10.1164/rccm.201610-2156SO.

[2] J. R. Beitler, A. Malhotra, and B. T. Thompson. "Ventilator-induced Lung Injury". In: *Clin Chest Med* 37.4 (2016), pp. 633–646. ISSN: 1557-8216 (Electronic) 0272-5231 (Linking). DOI: 10.1016/j.ccm.2016.07.004.

[3] M B Amato. "Effect of a protective-ventilation strategy on mortality in the acute respiratory distress syndrome". In: *N Engl J Med* 338.6 (1998), pp. 347–54. ISSN: 0028-4793. DOI: 10.1056/nejm199802053380602.

[4] J. J. Rouby et al. "Mechanical ventilation in patients with acute respiratory distress syndrome". In: *Anesthesiology* 101.1 (2004), pp. 228–34. ISSN: 0003-3022 (Print) 0003-3022 (Linking). DOI: 10.1097/00000542-200407000-00033.

[5] E. Frazee and K. Kashani. "Fluid Management for Critically Ill Patients: A Review of the Current State of Fluid Therapy in the Intensive Care Unit". In: *Kidney Dis (Basel)* 2.2 (2016), pp. 64–71. ISSN: 2296-9381 (Print) 2296-9357 (Linking). DOI: 10.1159/000446265.

[6] P. L. Marino. *The ICU book*. 2007.

[7] E. Akoumianaki et al. "The application of esophageal pressure measurement in patients with respiratory failure". In: *Am J Respir Crit Care Med* 189.5 (2014), pp. 520–31. ISSN: 1535-4970 (Electronic) 1073-449X (Linking). DOI: 10.1164/rccm.201312-2193CI.

[8] Hubmayr RD Loring SH Topulos GP. "Transpulmonary Pressure: The Importance of Precise Definitions and Limiting Assumptions." In: *Am J Respir Crit Care Med* 194.12 (2016), pp. 1452–1457. DOI: 10.1164/rccm.201512-2448CP.

[9] M. O. Fiedler et al. "Prospective Observational Study to Evaluate the Effect of Different Levels of Positive End-Expiratory Pressure on Lung Mechanics in Patients with and without Acute Respiratory Distress Syndrome". In: *J Clin Med* 9.8 (2020). ISSN: 2077-0383 (Print) 2077-0383. DOI: 10.3390/jcm9082446.

[10] J. R. Beitler et al. "Volume Delivered During Recruitment Maneuver Predicts Lung Stress in Acute Respiratory Distress Syndrome". In: *Crit Care Med* 44.1 (2016), pp. 91–9. ISSN: 0090-3493 (Print) 0090-3493. DOI: 10.1097/ccm.0000000000001355.

[11] J. R. Beitler et al. "Effect of Titrating Positive End-Expiratory Pressure (PEEP) With an Esophageal Pressure-Guided Strategy vs an Empirical High PEEP-Fio2 Strategy on Death and Days Free From Mechanical Ventilation Among Patients With Acute Respiratory Distress Syndrome: A Randomized Clinical Trial". In: *Jama* 321.9 (2019), pp. 846–857. ISSN: 0098-7484 (Print) 0098-7484. DOI: 10.1001/jama.2019.0555.

[12] R. Wang et al. "Mechanical Ventilation Strategy Guided by Transpulmonary Pressure in Severe Acute Respiratory Distress Syndrome Treated With Venovenous Extracorporeal Membrane Oxygenation". In: *Crit Care Med* 48.9 (2020), pp. 1280–1288. ISSN: 0090-3493. DOI: 10.1097/ccm.0000000000004445.

[13] E. Fernandez-Mondejar, F. Guerrero-Lopez, and M. Colmenero. "How important is the measurement of extravascular lung water?" In: *Curr Opin Crit Care* 13.1 (2007), pp. 79–83. ISSN: 1070-5295 (Print) 1070-5295 (Linking). DOI: 10.1097/MCC.0b013e328011459b.

[14] E. Fernandez-Mondejar et al. "Small increases in extravascular lung water are accurately detected by transpulmonary thermodilution". In: *J Trauma* 59.6 (2005), 1420–3, discussion 1424. ISSN: 0022-5282 (Print) 0022-5282 (Linking). DOI: 10.1097/01.ta.0000198360.01080.42.

[15] M. Jozwiak, J. L. Teboul, and X. Monnet. "Extravascular lung water in critical care: recent advances and clinical applications". In: *Ann Intensive Care* 5.1 (2015), p. 38. ISSN: 2110-5820 (Print) 2110-5820 (Linking). DOI: 10.1186/s13613-015-0081-9.

[16] A. Bhattacharjee et al. "How Useful is Extravascular Lung Water Measurement in Managing Lung Injury in Intensive Care Unit?" In: *Indian J Crit Care Med* 21.8 (2017), pp. 494–499. ISSN: 0972-5229 (Print) 0972-5229. DOI: 10.4103/ijccm.IJCCM_40_17.

[17] M. S. Chew et al. "Extravascular lung water index improves the diagnostic accuracy of lung injury in patients with shock". In: *Crit Care* 16.1 (2012), R1. ISSN: 1364-8535 (Print) 1364-8535. DOI: 10.1186/cc10599.

[18] T. R. Craig et al. “Extravascular lung water indexed to predicted body weight is a novel predictor of intensive care unit mortality in patients with acute lung injury”. In: *Crit Care Med* 38.1 (2010), pp. 114–20. ISSN: 0090-3493. DOI: 10.1097/CCM.0b013e3181b43050.

[19] M. Jozwiak et al. “Extravascular lung water is an independent prognostic factor in patients with acute respiratory distress syndrome”. In: *Crit Care Med* 41.2 (2013), pp. 472–80. ISSN: 0090-3493. DOI: 10.1097/CCM.0b013e31826ab377.

[20] S. Kushimoto et al. “Relationship between extravascular lung water and severity categories of acute respiratory distress syndrome by the Berlin definition”. In: *Crit Care* 17.4 (2013), R132. ISSN: 1364-8535 (Print) 1364-8535. DOI: 10.1186/cc12811.

[21] S. Kushimoto et al. “The clinical usefulness of extravascular lung water and pulmonary vascular permeability index to diagnose and characterize pulmonary edema: a prospective multicenter study on the quantitative differential diagnostic definition for acute lung injury/acute respiratory distress syndrome”. In: *Crit Care* 16.6 (2012), R232. ISSN: 1364-8535 (Print) 1364-8535. DOI: 10.1186/cc11898.

[22] K. Morisawa et al. “Difference in pulmonary permeability between indirect and direct acute respiratory distress syndrome assessed by the transpulmonary thermodilution technique: a prospective, observational, multi-institutional study”. In: *J Intensive Care* 2.1 (2014), p. 24. ISSN: 2052-0492 (Print) 2052-0492. DOI: 10.1186/2052-0492-2-24.

[23] R. Shi et al. “COVID-19 ARDS is characterized by higher extravascular lung water than non-COVID-19 ARDS: the PiCCOVID study”. In: *Crit Care* 25.1 (2021), p. 186. ISSN: 1364-8535 (Print) 1364-8535. DOI: 10.1186/s13054-021-03594-6.

[24] E. Virot et al. “Characterization of pulmonary impairment associated with COVID-19 in patients requiring mechanical ventilation”. In: *Rev Bras Ter Intensiva* 33.1 (2021), pp. 75–81. ISSN: 0103-507X (Print) 0103-507x. DOI: 10.5935/0103-507x.20210007.

[25] S. Rasch et al. “Increased extravascular lung water index (EVLWI) reflects rapid non-cardiogenic oedema and mortality in COVID-19 associated ARDS”. In: *Sci Rep* 11.1 (2021), p. 11524. ISSN: 2045-2322. DOI: 10.1038/s41598-021-91043-3.

[26] J. L. LeTourneau, J. Pinney, and C. R. Phillips. “Extravascular lung water predicts progression to acute lung injury in patients with increased risk*”. In: *Crit Care Med* 40.3 (2012), pp. 847–54. ISSN: 0090-3493 (Print) 0090-3493. DOI: 10.1097/CCM.0b013e318236f60e.

[27] J. Mallat et al. “Extravascular lung water indexed or not to predicted body weight is a predictor of mortality in septic shock patients”. In: *J Crit Care* 27.4 (2012), pp. 376–83. ISSN: 0883-9441. DOI: 10.1016/j.jcrc.2012.03.009.

[28] H. Wang et al. “Prognostic value of extravascular lung water and its potential role in guiding fluid therapy in septic shock after initial resuscitation”. In: *J Crit Care* 33 (2016), pp. 106–13. ISSN: 0883-9441. DOI: 10.1016/j.jcrc.2016.02.011.

[29] B. Wernly et al. “Extravascular lung water index and Halperin score to predict outcome in critically ill patients”. In: *Wien Klin Wochenschr* 130.17-18 (2018), pp. 505–510. ISSN: 0043-5325. DOI: 10.1007/s00508-018-1370-8.

[30] C. Cordemans et al. “Fluid management in critically ill patients: the role of extravascular lung water, abdominal hypertension, capillary leak, and fluid balance”. In: *Ann Intensive Care* 2.Suppl 1 Diagnosis and management of intra-abdominal hyperten (2012), S1. ISSN: 2110-5820 (Print) 2110-5820. DOI: 10.1186/2110-5820-2-s1-s1.

[31] F. Compton et al. “Changes in volumetric hemodynamic parameters induced by fluid removal on hemodialysis in critically ill patients”. In: *Ther Apher Dial* 19.1 (2015), pp. 23–9. ISSN: 1744-9979. DOI: 10.1111/1744-9987.12193.

[32] I. De Laet et al. “Renal replacement therapy with net fluid removal lowers intra-abdominal pressure and volumetric indices in critically ill patients”. In: *Ann Intensive Care* 2 Suppl 1.Suppl 1 (2012), S20. ISSN: 2110-5820 (Print) 2110-5820. DOI: 10.1186/2110-5820-2-s1-s20.

[33] F. Gavelli et al. “Transpulmonary thermodilution detects rapid and reversible increases in lung water induced by positive end-expiratory pressure in acute respiratory distress syndrome”. In: *Ann Intensive Care* 10.1 (2020), p. 28. ISSN: 2110-5820 (Print) 2110-5820. DOI: 10.1186/s13613-020-0644-2.

[34] B. Saugel et al. “Impact of large-volume thoracentesis on transpulmonary thermodilution-derived extravascular lung water in medical intensive care unit patients”. In: *J Crit Care* 28.2 (2013), pp. 196–201. ISSN: 0883-9441. DOI: 10.1016/j.jcrc.2012.05.002.

[35] A. A. Smetkin et al. “Increased extravascular lung water reduces the efficacy of alveolar recruitment maneuver in acute respiratory distress syndrome”. In: *Crit Care Res Pract* 2012 (2012), p. 606528. ISSN: 2090-1305 (Print) 2090-1305. DOI: 10.1155/2012/606528.

[36] J. G. Zhang et al. “Lung recruitment maneuver effects on respiratory mechanics and extravascular lung water index in patients with acute respiratory distress syndrome”. In: *World J Emerg Med* 2.3 (2011), pp. 201–5. ISSN: 1920-8642 (Print) 1920-8642. DOI: 10.5847/wjem.j.1920-8642.2011.03.008.

[37] M. Dres et al. “Extravascular lung water, B-type natriuretic peptide, and blood volume contraction enable diagnosis of weaning-induced pulmonary edema”. In: *Crit Care Med* 42.8 (2014), pp. 1882–9. ISSN: 0090-3493. DOI: 10.1097/ccm.0000000000000295.

[38] S. Liu et al. “Identification of regional overdistension, recruitment and cyclic alveolar collapse with electrical impedance tomography in an experimental ARDS model”. In: *Crit Care* 20.1 (2016), p. 119. ISSN: 1466-609X (Electronic) 1364-8535 (Linking). DOI: 10.1186/s13054-016-1300-y.

[39] T. Becher et al. “Individualization of PEEP and tidal volume in ARDS patients with electrical impedance tomography: a pilot feasibility study”. In: *Ann Intensive Care* 11.1 (2021), p. 89. ISSN: 2110-5820 (Print) 2110-5820. DOI: 10.1186/s13613-021-00877-7.

[40] I. G. Bikker et al. “Bedside measurement of changes in lung impedance to monitor alveolar ventilation in dependent and non-dependent parts by electrical impedance tomography during a positive end-expiratory pressure trial in mechanically ventilated intensive care unit patients”. In: *Crit Care* 14.3 (2010), R100. ISSN: 1364-8535 (Print) 1364-8535. DOI: 10.1186/cc9036.

[41] P. Blankman et al. “Detection of ’best’ positive end-expiratory pressure derived from electrical impedance tomography parameters during a decremental positive end-expiratory pressure trial”. In: *Crit Care* 18.3 (2014), R95. ISSN: 1364-8535 (Print) 1364-8535. DOI: 10.1186/cc13866.

[42] P. Blankman et al. “Detection of optimal PEEP for equal distribution of tidal volume by volumetric capnography and electrical impedance tomography during decreasing levels of PEEP in post cardiac-surgery patients”. In: *Br J Anaesth* 116.6 (2016), pp. 862–9. ISSN: 0007-0912 (Print) 0007-0912. DOI: 10.1093/bja/aew116.

[43] C. Grivans et al. “Positive end-expiratory pressure-induced changes in end-expiratory lung volume measured by spirometry and electric impedance tomography”. In: *Acta Anaesthesiol Scand* 55.9 (2011), pp. 1068–77. ISSN: 0001-5172. DOI: 10.1111/j.1399-6576.2011.02511.x.

[44] J. Karsten et al. “Positive end-expiratory pressure titration at bedside using electrical impedance tomography in post-operative cardiac surgery patients”. In: *Acta Anaesthesiol Scand* 59.6 (2015), pp. 723–32. ISSN: 0001-5172. DOI: 10.1111/aas.12518.

[45] K. Lowhagen, S. Lundin, and O. Stenqvist. “Regional intratidal gas distribution in acute lung injury and acute respiratory distress syndrome assessed by electric impedance tomography”. In: *Minerva Anestesiol* 76.12 (2010), pp. 1024–35. ISSN: 0375-9393.

[46] K. Lowhagen et al. “Prolonged moderate pressure recruitment manoeuvre results in lower optimal positive end-expiratory pressure and plateau pressure”. In: *Acta Anaesthesiol Scand* 55.2 (2011), pp. 175–84. ISSN: 0001-5172. DOI: 10.1111/j.1399-6576.2010.02366.x.

[47] K. Lowhagen et al. “A new non-radiological method to assess potential lung recruitability: a pilot study in ALI patients”. In: *Acta Anaesthesiol Scand* 55.2 (2011), pp. 165–74. ISSN: 0001-5172. DOI: 10.1111/j.1399-6576.2010.02331.x.

[48] M. Mlček et al. “Targeted lateral positioning decreases lung collapse and overdistension in COVID-19-associated ARDS”. In: *BMC Pulm Med* 21.1 (2021), p. 133. ISSN: 1471-2466. DOI: 10.1186/s12890-021-01501-x.

[49] S. Pulletz et al. “Regional lung opening and closing pressures in patients with acute lung injury”. In: *J Crit Care* 27.3 (2012), 323.e11–8. ISSN: 0883-9441. DOI: 10.1016/j.jcrc.2011.09.002.

[50] T. Mauri et al. “Bedside assessment of the effects of positive end-expiratory pressure on lung inflation and recruitment by the helium dilution technique and electrical impedance tomography”. In: *Intensive Care Med* 42.10 (2016), pp. 1576–1587. ISSN: 0342-4642. DOI: 10.1007/s00134-016-4467-4.

[51] C. Gómez-Laberge, J. H. Arnold, and G. K. Wolf. “A unified approach for EIT imaging of regional overdistension and atelectasis in acute lung injury”. In: *IEEE Trans Med Imaging* 31.3 (2012), pp. 834–42. ISSN: 0278-0062 (Print) 0278-0062. DOI: 10.1109/tmi.2012.2183641.

[52] F. Dalla Corte et al. “Dynamic bedside assessment of the physiologic effects of prone position in acute respiratory distress syndrome patients by electrical impedance tomography”. In: *Minerva Anestesiol* 86.10 (2020), pp. 1057–1064. ISSN: 0375-9393. DOI: 10.23736/s0375-9393.20.14130-0.

[53] T. Bein et al. “No change in the regional distribution of tidal volume during lateral posture in mechanically ventilated patients assessed by electrical impedance tomography”. In: *Clin Physiol Funct Imaging* 30.4 (2010), pp. 234–40. ISSN: 1475-0961 (Print) 1475-0961. DOI: 10.1111/j.1475-097X.2010.00933.x.

[54] R. Cornejo et al. “Estimation of changes in cyclic lung strain by electrical impedance tomography: Proof-of-concept study”. In: *Acta Anaesthesiol Scand* 65.2 (2021), pp. 228–235. ISSN: 0001-5172. DOI: 10.1111/aas.13723.

[55] A. Anile et al. “A simplified lung ultrasound approach to detect increased extravascular lung water in critically ill patients”. In: *Crit Ultrasound J* 9.1 (2017), p. 13. ISSN: 2036-3176 (Print) 2036-3176. DOI: 10.1186/s13089-017-0068-x.

[56] G. Baldi et al. “Lung water assessment by lung ultrasonography in intensive care: a pilot study”. In: *Intensive Care Med* 39.1 (2013), pp. 74–84. ISSN: 0342-4642. DOI: 10.1007/s00134-012-2694-x.

[57] F. Bilotta et al. “Ultrasound imaging and use of B-lines for functional lung evaluation in neurocritical care: a prospective, observational study”. In: *Eur J Anaesthesiol* 30.8 (2013), pp. 464–8. ISSN: 0265-0215. DOI: 10.1097/EJA.0b013e32835fe4a4.

[58] B. Bouhemad et al. “Bedside ultrasound assessment of positive end-expiratory pressure-induced lung recruitment”. In: *Am J Respir Crit Care Med* 183.3 (2011), pp. 341–7. ISSN: 1073-449x. DOI: 10.1164/rccm.201003-0369OC.

[59] C. Brusasco et al. “Quantitative lung ultrasonography: a putative new algorithm for automatic detection and quantification of B-lines”. In: *Crit Care* 23.1 (2019), p. 288. ISSN: 1364-8535 (Print) 1364-8535. DOI: 10.1186/s13054-019-2569-4.

[60] A. Ciumanghel et al. “B-lines score on lung ultrasound as a direct measure of respiratory dysfunction in ICU patients with acute kidney injury”. In: *Int Urol Nephrol* 50.1 (2018), pp. 113–119. ISSN: 0301-1623. DOI: 10.1007/s11255-017-1730-8.

[61] F. Corradi et al. “Computer-Aided Quantitative Ultrasonography for Detection of Pulmonary Edema in Mechanically Ventilated Cardiac Surgery Patients”. In: *Chest* 150.3 (2016), pp. 640–51. ISSN: 0012-3692. DOI: 10.1016/j.chest.2016.04.013.

[62] P. Enghard et al. “Simplified lung ultrasound protocol shows excellent prediction of extravascular lung water in ventilated intensive care patients”. In: *Crit Care* 19.1 (2015), p. 36. ISSN: 1364-8535 (Print) 1364-8535. DOI: 10.1186/s13054-015-0756-5.

[63] A. Ferré et al. “Lung ultrasound allows the diagnosis of weaning-induced pulmonary oedema”. In: *Intensive Care Med* 45.5 (2019), pp. 601–608. ISSN: 0342-4642. DOI: 10.1007/s00134-019-05573-6.

[64] V. Gattupalli, K. Jain, and T. Samra. “Lung Ultrasound as a Bedside Tool for Assessment of Extravascular Lung Water in Critically Ill Head Injured Patients: An Observational Study”. In: *Indian J Crit Care Med* 23.3 (2019), pp. 131–134. ISSN: 0972-5229 (Print) 0972-5229. DOI: 10.5005/jp-journals-10071-23135.

[65] U. Mayr et al. “B-Lines Scores Derived From Lung Ultrasound Provide Accurate Prediction of Extravascular Lung Water Index: An Observational Study in Critically Ill Patients”. In: *J Intensive Care Med* (2020), p. 885066620967655. ISSN: 0885-0666. DOI: 10.1177/0885066620967655.

[66] K. L. Mendrala et al. “Comparing transpulmonary thermodilution monitoring to lung ultrasound during pneumonia: an observational study”. In: *Adv Respir Med* (2018). ISSN: 2451-4934. DOI: 10.5603/ARM.a2018.0045.

[67] D. M. Rusu et al. “Lung Ultrasound-Guided Fluid Management versus Standard Care in Surgical ICU Patients: A Randomised Controlled Trial”. In: *Diagnostics (Basel)* 11.8 (2021). ISSN: 2075-4418 (Print) 2075-4418. DOI: 10.3390/diagnostics11081444.

[68] G. Volpicelli et al. “Lung ultrasound predicts well extravascular lung water but is of limited usefulness in the prediction of wedge pressure”. In: *Anesthesiology* 121.2 (2014), pp. 320–7. ISSN: 0003-3022. DOI: 10.1097/aln.0000000000000300.

[69] Z. Zhao et al. “Prognostic value of extravascular lung water assessed with lung ultrasound score by chest sonography in patients with acute respiratory distress syndrome”. In: *BMC Pulm Med* 15 (2015), p. 98. ISSN: 1471-2466. DOI: 10.1186/s12890-015-0091-2.

[70] M. Danish et al. “Diagnostic Performance of 6-Point Lung Ultrasound in ICU Patients: A Comparison with Chest X-Ray and CT Thorax”. In: *Turk J Anaesthesiol Reanim* 47.4 (2019), pp. 307–319. ISSN: 2667-677X (Print) 2149-276x. DOI: 10.5152/tjar.2019.73603.

[71] B. Bataille et al. “Accuracy of ultrasound B-lines score and E/Ea ratio to estimate extravascular lung water and its variations in patients with acute respiratory distress syndrome”. In: *J Clin Monit Comput* 29.1 (2015), pp. 169–76. ISSN: 1387-1307. DOI: 10.1007/s10877-014-9582-6.

[72] B. Rode et al. “Positive end-expiratory pressure lung recruitment: comparison between lower inflection point and ultrasound assessment”. In: *Wien Klin Wochenschr* 124.23-24 (2012), pp. 842–7. ISSN: 0043-5325. DOI: 10.1007/s00508-012-0303-1.

[73] C. Brusasco et al. “Second-order grey-scale texture analysis of pleural ultrasound images to differentiate acute respiratory distress syndrome and cardiogenic pulmonary edema”. In: *J Clin Monit Comput* (2020). ISSN: 1387-1307. DOI: 10.1007/s10877-020-00629-1.

[74] G. Duclos et al. “Speckle tracking quantification of lung sliding for the diagnosis of pneumothorax: a multicentric observational study”. In: *Intensive Care Med* 45.9 (2019), pp. 1212–1218. ISSN: 0342-4642. DOI: 10.1007/s00134-019-05710-1.

[75] E. Fissore et al. “Pneumothorax diagnosis with lung sliding quantification by speckle tracking: A prospective multicentric observational study”. In: *Am J Emerg Med* 49 (2021), pp. 14–17. ISSN: 0735-6757. DOI: 10.1016/j.ajem.2021.05.022.

[76] B. Ziapour and H. S. Haji. “”Anterior convergent” chest probing in rapid ultrasound transducer positioning versus formal chest ultrasonography to detect pneumothorax during the primary survey of hospital trauma patients: a diagnostic accuracy study”. In: *J Trauma Manag Outcomes* 9 (2015), p. 9. ISSN: 1752-2897 (Print) 1752-2897. DOI: 10.1186/s13032-015-0030-5.

[77] S. Mondillo et al. “Speckle-tracking echocardiography: a new technique for assessing myocardial function”. In: *J Ultrasound Med* 30.1 (2011), pp. 71–83. ISSN: 1550-9613 (Electronic) 0278-4297 (Linking). DOI: 10.7863/jum.2011.30.1.71.

[78] A. Alharthy et al. “Residual Lung Injury in Patients Recovering From COVID-19 Critical Illness: A Prospective Longitudinal Point-of-Care Lung Ultrasound Study”. In: *J Ultrasound Med* 40.9 (2021), pp. 1823–1838. ISSN: 0278-4297. DOI: 10.1002/jum.15563.

[79] M. E. Haaksma et al. “Lung ultrasound findings in patients with novel SARS-CoV-2”. In: *ERJ Open Res* 6.4 (2020). ISSN: 2312-0541 (Print) 2312-0541. DOI: 10.1183/23120541.00238-2020.

[80] J. Rubio-Gracia et al. “Point-of-care lung ultrasound assessment for risk stratification and therapy guiding in COVID-19 patients. A prospective non-interventional study”. In: *Eur Respir J* (2021). ISSN: 0903-1936 (Print) 0903-1936. DOI: 10.1183/13993003.04283-2020.

[81] G. Secco et al. “Can Alveolar-Arterial Difference and Lung Ultrasound Help the Clinical Decision Making in Patients with COVID-19?” In: *Diagnostics (Basel)* 11.5 (2021). ISSN: 2075-4418 (Print) 2075-4418. DOI: 10.3390/diagnostics11050761.

[82] M. Garnier et al. “Morpho-functional evaluation of lung aeration as a marker of sickle-cell acute chest syndrome severity in the ICU: a prospective cohort study”. In: *Ann Intensive Care* 9.1 (2019), p. 109. ISSN: 2110-5820 (Print) 2110-5820. DOI: 10.1186/s13613-019-0583-y.

[83] T. Schepens et al. “The course of diaphragm atrophy in ventilated patients assessed with ultrasound: a longitudinal cohort study”. In: *Crit Care* 19 (2015), p. 422. ISSN: 1364-8535 (Print) 1364-8535. DOI: 10.1186/s13054-015-1141-0.

[84] G. Ntoumenopoulos, H. Buscher, and S. Scott. “Lung ultrasound score as an indicator of dynamic lung compliance during veno-venous extra-corporeal membrane oxygenation”. In: *Int J Artif Organs* 44.3 (2021), pp. 194–198. ISSN: 0391-3988. DOI: 10.1177/0391398820948870.

[85] P. Shen et al. “Dynamic assessment of lung injury by ultrasound in patients with acute paraquat poisoning”. In: *J Int Med Res* 48.5 (2020), p. 300060520920435. ISSN: 0300-0605 (Print) 0300-0605. DOI: 10.1177/0300060520920435.

[86] J. M. Constantin et al. “Personalised mechanical ventilation tailored to lung morphology versus low positive end-expiratory pressure for patients with acute respiratory distress syndrome in France (the LIVE study): a multicentre, single-blind, randomised controlled trial”. In: *Lancet Respir Med* 7.10 (2019), pp. 870–880. ISSN: 2213-2619 (Electronic) 2213-2600 (Linking). DOI: 10.1016/S2213-2600(19)30138-9.

Appendix A: Searchterm MEDLINE

((("Respiration, Artificial"[Mesh] OR "Mechanical Ventilation"[tw] OR "Artificial Respiration"[tw] OR "High-Frequency Ventilation"[tw] OR "High-Frequency Jet Ventilation"[tw] OR "Interactive Ventilatory Support"[tw] OR "Liquid Ventilation"[tw] OR "Noninvasive Ventilation"[tw] OR "One-Lung Ventilation"[tw] OR "Positive-Pressure Respiration"[tw] OR "Continuous Positive Airway Pressure"[tw] OR "Intermittent Positive-Pressure Breathing"[tw] OR "Intermittent Positive-Pressure Ventilation"[tw] OR "Ventilator Weaning"[tw] OR "Intensive Care Units"[Mesh] OR "ICU"[tw] OR "ICUs"[tw] OR "Intensive Care"[tw] OR "Critical Care"[Mesh] OR "Critical Care"[tw] OR "Pneumothorax"[majr] OR "Pneumothorax"[ti]) AND ("Lung Injury"[Mesh] OR "lung injury"[tw] OR "Pulmonary Injury"[tw] OR "Pulmonary Injuries"[tw] OR "Lung Injuries"[tw] OR "Meconium Aspiration Syndrome"[tw] OR "Pneumoconiosis"[tw] OR "Anthracosis"[tw] OR "Anthracosilicosis"[tw] OR "Asbestosis"[tw] OR "Berylliosis"[tw] OR "Byssinosis"[tw] OR "Caplan Syndrome"[tw] OR "Siderosis"[tw] OR "Silicosis"[tw] OR "Silicotuberculosis"[tw] OR "Radiation Pneumonitis"[tw] OR "Ventilator-Induced Lung Injury"[tw] OR "Bronchopulmonary Dysplasia"[tw] OR "Extravascular Lung Water"[Mesh] OR "lung water"[tw] OR "lung sliding"[tw] OR "nonventilatory parameters"[tw]) AND ("Ultrasonography"[Mesh] OR "Ultrasonics"[Mesh] OR "ultrasound"[tw] OR "Ultrasonography"[tw] OR "Ultraso*"[tw] OR "sonogra*"[tw] OR "echogra*"[tw] OR "transpulmonary measure*"[tw] OR "transpulmonary"[tw] OR (("Extravascular Lung Water"[Mesh] OR "Extravascular lung water"[tw]) AND ("measurement"[tw] OR "measur*"[tw])) OR "Electrical impedance tomography"[tw] OR "Electric impedance tomography"[tw] OR (("Electric Impedance"[Mesh] OR "Electric Impedance"[tw] OR "Electrical Impedance"[tw]) AND ("Tomography"[Mesh] OR "Tomography"[tw] OR "Tomogr*"[tw])) OR "transpulmonary pressure"[tw] OR "pleural pressure"[tw] OR "esophagus balloon"[tw] OR (("esophagus"[tw] OR "oesophagus"[tw]) AND ("balloon"[tw] OR "balloons"[tw])) OR (("extravascular fluid "[tw] OR "extravascular lung water"[tw] OR "extravascular water"[tw]) AND ("measurement"[tw] OR "measur*"[tw]))) NOT ("Animals"[mesh] NOT "Humans"[mesh])) OR (("Respiration, Artificial"[Mesh] OR "Mechanical Ventilation"[tw] OR "Artificial Respiration"[tw] OR "High-Frequency Ventilation"[tw] OR "High-Frequency Jet Ventilation"[tw] OR "Interactive Ventilatory Support"[tw] OR "Liquid Ventilation"[tw] OR "Noninvasive Ventilation"[tw] OR "One-Lung Ventilation"[tw] OR "Positive-Pressure Respiration"[tw] OR "Continuous Positive Airway Pressure"[tw] OR "Intermittent Positive-Pressure Breathing"[tw] OR "Intermittent Positive-Pressure Ventilation"[tw] OR "Ventilator Weaning"[tw]) AND ("Intensive Care Units"[Mesh] OR "ICU"[tw] OR "ICUs"[tw] OR "Intensive Care"[tw] OR "Critical Care"[Mesh] OR "Critical Care"[tw]) AND ("Lung Injury"[Mesh] OR "lung injury"[tw] OR "Pulmonary Injury"[tw] OR "Pulmonary Injuries"[tw] OR "Lung Injuries"[tw] OR "Meconium Aspiration Syndrome"[tw] OR "Pneumoconiosis"[tw] OR "Anthracosis"[tw] OR "Anthracosilicosis"[tw] OR "Asbestosis"[tw] OR "Berylliosis"[tw] OR "Byssinosis"[tw] OR "Caplan Syndrome"[tw] OR "Siderosis"[tw] OR "Silicosis"[tw] OR "Silicotuberculosis"[tw] OR "Radiation Pneumonitis"[tw] OR "Ventilator-Induced Lung Injury"[tw] OR "Bronchopulmonary Dysplasia"[tw] OR "Extravascular Lung Water"[Mesh] OR "lung water"[tw] OR "lung sliding"[tw] OR "nonventilatory parameters"[tw]) AND ("Ultrasonography"[Mesh] OR "Ultrasonics"[Mesh] OR "ultrasound"[tw] OR "Ultrasonography"[tw] OR "Ultraso*"[tw] OR "sonogra*"[tw] OR "echogra*"[tw] OR "transpulmonary measure*"[tw] OR "transpulmonary"[tw] OR (("Extravascular Lung Water"[Mesh] OR "Extravascular lung water"[tw]) AND ("measurement"[tw] OR "measur*"[tw])) OR "Electrical impedance tomography"[tw] OR "Electric impedance tomography"[tw] OR (("Electric Impedance"[Mesh] OR "Electric Impedance"[tw] OR "Electrical Impedance"[tw]) AND ("Tomography"[Mesh] OR "Tomography"[tw] OR "Tomogr*"[tw])) OR "transpulmonary pressure"[tw] OR "pleural pressure"[tw] OR "esophagus balloon"[tw] OR (("esophagus"[tw] OR "oesophagus"[tw]) AND ("balloon"[tw] OR "balloons"[tw])) OR (("extravascular fluid "[tw] OR "extravascular lung water"[tw] OR "extravascular water"[tw]) AND ("measurement"[tw] OR "measur*"[tw])) OR "measur*"[ti] OR "Diagnostic Imaging"[majr] OR "Lung Injury/diagnostic imaging"[majr]) NOT ("Animals"[mesh] NOT "Humans"[mesh]))) AND ("2009/12/31"[PDAT] : "3000/12/31"[PDAT]) AND english[la] NOT (("Review"[ptyp] OR "review"[ti]) NOT ("Clinical Study"[ptyp] OR "trial"[ti] OR "RCT"[ti]))

A2. Typical mistakes

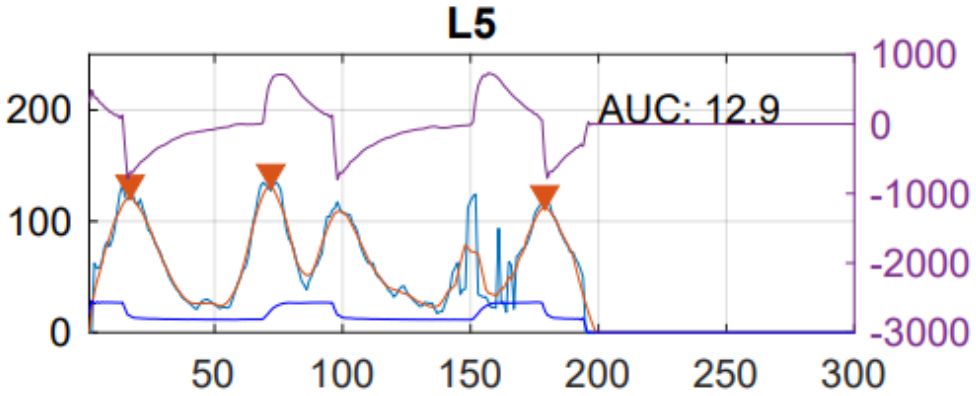

Figure A2-1: Signal underestimation due to a real time segmentation error.

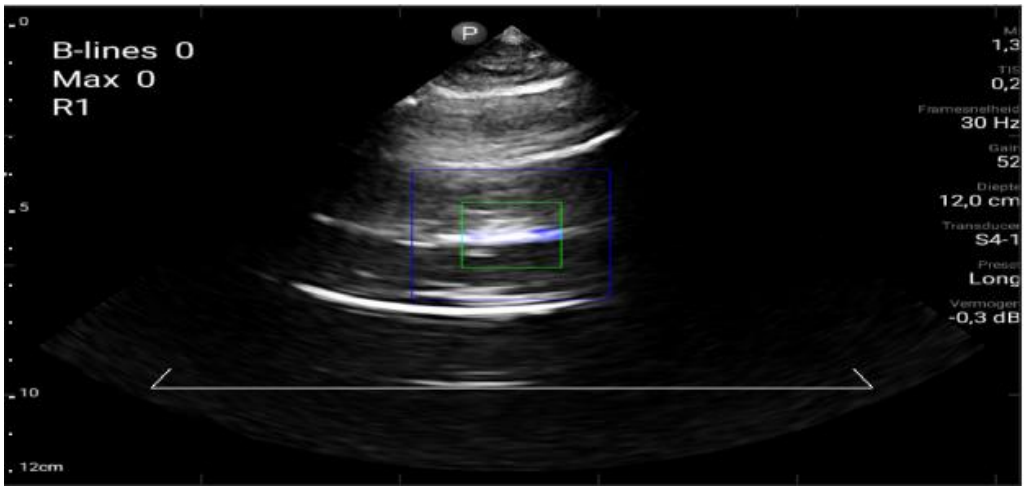

Figure A2-2: Initial pleural segmentation mistake: Segmentation of A-line.

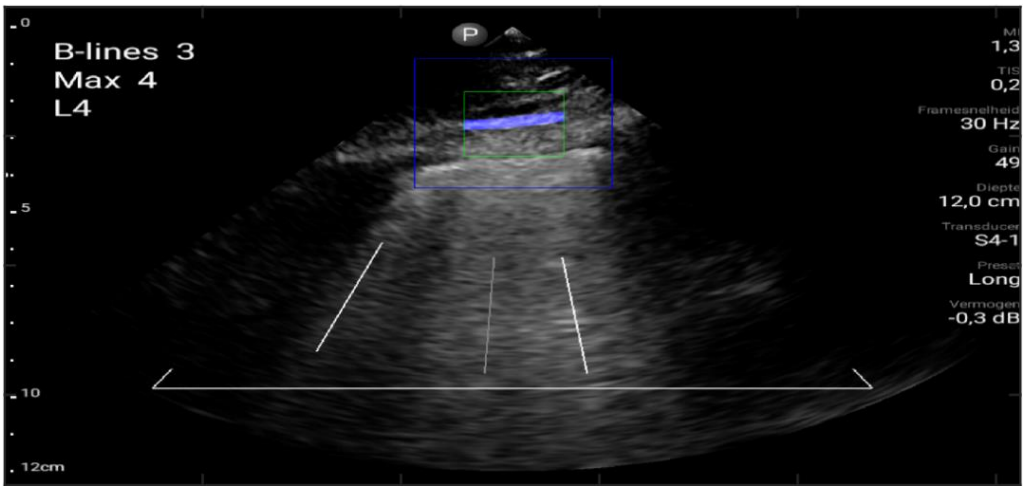

Figure A2-3: Initial pleural segmentation mistake: Segmentation of muscle.

A3. Ultrasound protocol UTOPIA study in COVID patients

Background and introduction

Mechanical ventilation is, albeit lifesaving, damaging to the lung and may result in ventilator induced lung injury (VILI). Patients who are mechanically ventilated and have underlying lung abnormalities, such as consolidations, atelectasis or ARDS may benefit from lung recruitment maneuvers and higher PEEP levels to open up the lung and keep it open. A lung recruitment maneuver will result in more open lung but may also result in overextension of healthy parts of lung which may damage these parts.

The prevention of VILI is currently an important topic in critical care. Esophageal pressure measurements has been studied as a tool to prevent VILI that represents the changes in pleural pressure. However, this technique cannot give a good approximation of regional overdistension due to the uneven distribution of air delivery in patients with acute lung injury. Regional overdistention is associated with higher mortality due to lung damage and possible activation of cytokine storm resulting in multi organ failure.

The holy grail of mechanical ventilation is therefore to find the ventilator setting which maximally opens the lung parts which are closed without overextending the lung parts which are open. Currently this may only be reliably done with serial CT scanning or impedance measurements. However, we believe that using ultrasound we may also be able to measure lung features regionally. Lung features are distinctive patterns in an image that could say something about the condition of the lung. One example is the B line quantification algorithms that quantify lung fluid by counting comet trails artefacts from the pleura. Using ultrasound, we may be able to ascertain whether lung parts that were closed become opened up by scoring the level of atelectasis, consolidations and open lung all over the lungs and we may be able to measure overextension of the already open lung parts by quantifying lung sliding using speckle tracking techniques. Lung sliding is dynamic hyperechoic line in the image that occurred due to the visceral pleura moves against the parietal pleura with respiration.

The study aims therefore to investigate the effects of PEEP on lung sliding with the goal to use ultrasound to optimize mechanical ventilation. Secondary aim is to extract additional features to monitor diagraph movement and strain for example. The research will take place at the Leiden University Medical Center (LUMC) at the Intensive Care department. The pilot study is a collaboration between the hospital LUMC and manufacturer Philips. Ultrasound (US) imaging is used to investigate lung physiology and mechanics and specifically lung sliding. US is a non-radiating imaging modality that uses ultrasonic sound waves to measure tissue density and is clinically proven safe for humans.

Method

COVID group:

Patient is confirmed correct sedated and laid in supine position. A Hamilton data recording device is attached to the ventilator and activated.

1. Place Hamilton dongle in the serial port of the Hamilton C6 ventilator. **Use only the dongle with the green cable!.**
2. Click on start
3. Switch to wave mode
4. Click on start
5. Lights goes off. After +- 15 sec a small flickering of light indicate correct functionality.

6. For the image acquisition, we use a lumify S4-1 transducer in combination with a Samsung galaxy tab that is registered as a medical device. **Use only the smaller tablet (These tablets can only export images from the USB C port)**. First step is to request a lung ultrasound from the commando centrum. Then select the **Lung preset** and Select the patient info in the tablet by clicking new patient and 'zoekresultaten'. Furthermore, Fill the research number (as shown in a table below in section Administration) in as addition to the patient information box 'description'. Choose B-line feature. Then, the acquisition will take place in the following order:

- R1 = Upper anterior right lung
- R2 = Lower anterior right lung
- R3 = Upper lateral right lung
- R4 = Lower lateral right lung
- R5 = Upper posterior right lung
- R6 = Lower posterior right lung
- RD = Diagraph image right lung
- L1 = Upper anterior left lung
- L2 = Lower anterior left lung
- L3 = Upper lateral left lung
- L4 = Lower lateral left lung
- L5 = Upper posterior left lung
- L6 = Lower posterior left lung
- LD = Diagraph image left lung

Please check every image with the location code! A graphical representation of the location codes are visible in figure 1.

The duration of each acquisition is 7 seconds (check the settings).

7. Export data to DICOM store.
8. Click stop on the Hamilton dongle and remove the dongle.
9. Clean patient and equipment.
10. Fill in all requested information in the table below in section administration.

The data from the lumify is extracted with a USB flash drive to a secured server at the end of the day. Than the USB drive is formatted correctly after use. Same applied for the ventilator data.

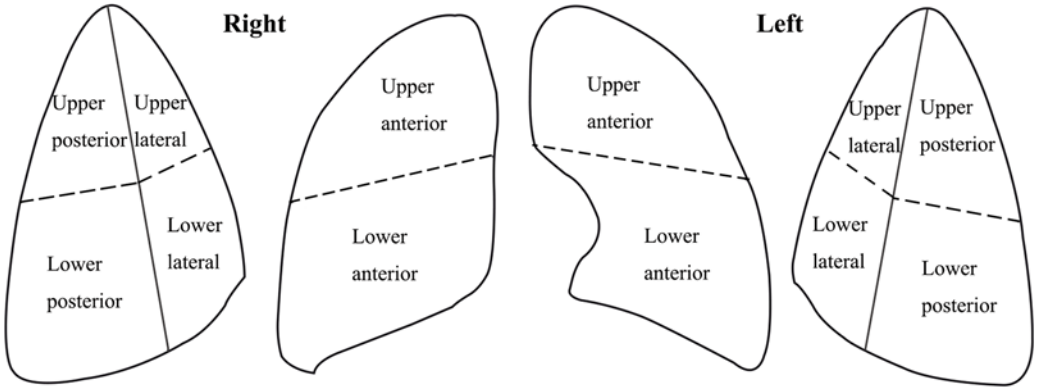

Figure 1: Each lung is separated into six quadrants: anterior, lateral and posterior zones that are further divided in an upper and lower zone. Image from Deng, Q., Cao, S., Wang, H. et al. Application of quantitative lung ultrasound instead of CT for monitoring COVID-19 pneumonia in pregnant women: a single-center retrospective study. BMC Pregnancy Childbirth 21, 259 (2021). https://doi.org/10.1186/s12884-021-03728-2

Administration

Research number	Date	Time (hh:mm)	Room number	Ventilator mode	Recruitment[1]	Diaphragm image (right,left,both,none)
R0005	18-11	13:30	8	SPONT	0	Right
R0006						
R0007						
R0008						

[1]Recruitment: 0 = without recruitment, 1= before recruitment, 2= during recruitment, 3 = 15 minutes after recruitment.

A4. CMUT ultrasound transducer patches for monitoring purpose

Recently, Philips developed the capitative micromachined ultrasonic transducer or so called CMUT chip. The chip is a breakthrough ultrasound technology that can be used to receive and transmit acoustic signals in the ultrasonic range. Conventional ultrasound probes consist of multiple rows of around 120 piezoelectric crystals (depending on the type of probe). Each crystal is wired to the connector making the connector clumping and big. The cable that connects the probe with the connector is heavily shielded to protect the small signals from getting disrupted. The ultrasound semiconductor does not use any crystals but instead uses capacitive zones integrated on a silicon chip. These capacitive zones or sensors can be used for sending and receiving sound waves using a radiofrequency (RF) pulse or RF measuring circuit applied to it. The sensors, wires, and computed circuits can be placed on the same chip making it very thin and cost-effective. The chips are manufactured using thin film photolithography, scanning, a well-known microfabrication that can be very cost-effective for mass production. Another advantage is the preprocessing ability of the integrated computational circuit. The computation circuit in the chip converts the raw data into a digital image. This results in fewer wires, just two for power and two for data communication. But also leads to less data interfering over the cable and the possibility of sending the data wirelessly when the chip is connected to an integrated battery. Due to the small form factor of the chip and special ultrasound gel, the ultrasound sensors can be attached to the human body for more than 48 hours, making it an ideal solution for continuous monitoring. Moreover, the sensors are small and inexpensive which would enable us in clinical practice to attach more than one sensor and monitor different locations simultaneously in real-time.

8. References

1. Beitler JR, Malhotra A, Thompson BT. Ventilator-induced Lung Injury. Clin Chest Med. 2016;37(4):633-46.
2. Amato MB, Barbas CS, Medeiros DM, Magaldi RB, Schettino GP, Lorenzi-Filho G, et al. Effect of a protective-ventilation strategy on mortality in the acute respiratory distress syndrome. N Engl J Med. 1998;338(6):347-54.
3. Halbertsma FJ, Vaneker M, Scheffer GJ, van der Hoeven JG. Cytokines and biotrauma in ventilator-induced lung injury: a critical review of the literature. Neth J Med. 2005;63(10):382-92.
4. Mauri T, Yoshida T, Bellani G, Goligher EC, Carteaux G, Rittayamai N, et al. Esophageal and transpulmonary pressure in the clinical setting: meaning, usefulness and perspectives. Intensive Care Medicine. 2016;42(9):1360-73.
5. Morgan M, Bell D. Ultrasound (introduction). Radiopaediaorg. 2022.
6. Nadrljanski M, Bell, D. . History of ultrasound in medicine. Radiopaediaorg. 2022.
7. Lichtenstein DA, Mezière GA. Relevance of lung ultrasound in the diagnosis of acute respiratory failure: the BLUE protocol. Chest. 2008;134(1):117-25.
8. Markota A, Golub J, Stožer A, Fluher J, Prosen G, Bergauer A, et al. Absence of lung sliding is not a reliable sign of pneumothorax in patients with high positive end-expiratory pressure. Am J Emerg Med. 2016;34(10):2034-6.
9. Mojoli F, Bouhemad B, Mongodi S, Lichtenstein D. Lung Ultrasound for Critically Ill Patients. Am J Respir Crit Care Med. 2019;199(6):701-14.
10. Duclos G, Bobbia X, Markarian T, Muller L, Cheyssac C, Castillon S, et al. Speckle tracking quantification of lung sliding for the diagnosis of pneumothorax: a multicentric observational study. Intensive Care Med. 2019;45(9):1212-8.
11. Dargent A, Chatelain E, Kreitmann L, Quenot J-P, Cour M, Argaud L, et al. Lung ultrasound score to monitor COVID-19 pneumonia progression in patients with ARDS. PLoS One. 2020;15(7):e0236312-e.
12. Deng Q, Cao S, Wang H, Zhang Y, Chen L, Yang Z, et al. Application of quantitative lung ultrasound instead of CT for monitoring COVID-19 pneumonia in pregnant women: a single-center retrospective study. BMC Pregnancy and Childbirth. 2021;21(1):259.
13. Marwick TH, Leano RL, Brown J, Sun J-P, Hoffmann R, Lysyansky P, et al. Myocardial Strain Measurement With 2-Dimensional Speckle-Tracking Echocardiography: Definition of Normal Range. JACC: Cardiovascular Imaging. 2009;2(1):80-4.
14. Mohamed A. Automated speckle tracking in ultrasound images of tendon movements. UK: University of Salford; 2015.
15. Garcia D, Lantelme P, Saloux E. Introduction to speckle tracking in cardiac ultrasound imaging. Handbook of speckle filtering and tracking in cardiovascular ultrasound imaging and video2018.
16. Jerman T, Pernuš F, Likar B, Ž Š. Enhancement of Vascular Structures in 3D and 2D Angiographic Images. IEEE Transactions on Medical Imaging. 2016;35(9):2107-18.
17. MATLAB. fitLME https://nl.mathworks.com/help/stats/fitlme.html2022
18. Fumagalli J, Santiago RRS, Teggia Droghi M, Zhang C, Fintelmann FJ, Troschel FM, et al. Lung Recruitment in Obese Patients with Acute Respiratory Distress Syndrome. Anesthesiology. 2019;130(5):791-803.
19. Costa ELV, Borges JB, Melo A, Suarez-Sipmann F, Toufen C, Bohm SH, et al. Bedside estimation of recruitable alveolar collapse and hyperdistension by electrical impedance tomography. Intensive Care Medicine. 2009;35(6):1132-7.
20. Zhou X, Zhou X, Leow CH, Tang MX. Measurement of Flow Volume in the Presence of Reverse Flow with Ultrasound Speckle Decorrelation. Ultrasound Med Biol. 2019;45(11):3056-66.

21. Grady L. Random walks for image segmentation. IEEE Trans Pattern Anal Mach Intell. 2006;28(11):1768-83.
22. Anantrasirichai N, Hayes W, Allinovi M, Bull D, Achim A. Line Detection as an Inverse Problem: Application to Lung Ultrasound Imaging. IEEE Trans Med Imaging. 2017;36(10):2045-56.
23. Kulhare S, Zheng X, Mehanian C, Gregory C, Zhu M, Gregory K, et al., editors. Ultrasound-Based Detection of Lung Abnormalities Using Single Shot Detection Convolutional Neural Networks2018; Cham: Springer International Publishing.
24. McDermott C, Łącki M, Sainsbury B, Henry J, Filippov M, Rossa C. Sonographic Diagnosis of COVID-19: A Review of Image Processing for Lung Ultrasound. Front Big Data. 2021;4:612561.
25. Lichtenstein DA. Lung ultrasound in the critically ill. Ann Intensive Care. 2014;4(1):1.
26. Victorino JA, Borges JB, Okamoto VN, Matos GF, Tucci MR, Caramez MP, et al. Imbalances in regional lung ventilation: a validation study on electrical impedance tomography. Am J Respir Crit Care Med. 2004;169(7):791-800.
27. Frerichs I, Hinz J, Herrmann P, Weisser G, Hahn G, Dudykevych T, et al. Detection of local lung air content by electrical impedance tomography compared with electron beam CT. J Appl Physiol (1985). 2002;93(2):660-6.
28. Richard JC, Pouzot C, Gros A, Tourevieille C, Lebars D, Lavenne F, et al. Electrical impedance tomography compared to positron emission tomography for the measurement of regional lung ventilation: an experimental study. Crit Care. 2009;13(3):R82.
29. Fissore E, Zieleskiewicz L, Markarian T, Muller L, Duclos G, Bourgoin M, et al. Pneumothorax diagnosis with lung sliding quantification by speckle tracking: A prospective multicentric observational study. Am J Emerg Med. 2021;49:14-7.
30. Rubin JM, Feng M, Hadley SW, Fowlkes JB, Hamilton JD. Potential use of ultrasound speckle tracking for motion management during radiotherapy: preliminary report. J Ultrasound Med. 2012;31(3):469-81.
31. Brusasco C, Santori G, Tavazzi G, Via G, Robba C, Gargani L, et al. Second-order grey-scale texture analysis of pleural ultrasound images to differentiate acute respiratory distress syndrome and cardiogenic pulmonary edema. Journal of Clinical Monitoring and Computing. 2020.